RUTHENIUM HALF-SANDWICH COMPLEXES CONTAINING NOVEL ANIONIC (PHOSPHINO)TETRAPHENYLBORATE LIGANDS

by

Timothy G. Larocque

Submitted to

The Department of Chemistry, Lakehead University

in Partial Fulfillment of the Requirements for

the Degree of Master of Science

Supervisor: Dr. G. J. Spivak

Department of Chemistry, Lakehead University

Thunder Bay, Ontario, Canada, P7B 5E1

August 2009

Abstract

In an attempt to expand upon previous work involving ruthenium-arene complexes bearing anionic (phosphino)tetraphenylborate ligands, $[PR_2(p\text{-}Ph_3BC_6H_4)]^-$, and possibly provide further insight into the products obtained, a series of metal complexes containing these anionic phosphines were synthesized. The newly synthesized complexes include $[E][RuCl_2(\eta^6\text{-}p\text{-cymene})\{PCy_2(p\text{-}Ph_3BC_6H_4)\}]$ ($E = PNP^+$, **1a**; Bu_4N^+, **1a′**) and $[E][RuCl_2(\eta^6\text{-}C_6H_6)\{PR_2(p\text{-}Ph_3BC_6H_4)\}]$ ($R = {}^iPr$, $E = PNP^+$, **4a**; $R = {}^iPr$, $E = Bu_4N^+$, **4a′**; R = Ph, $E = PNP^+$, **4b**; R = Ph, $E = Bu_4N^+$, **4b′**; R = Cy, $E = PNP^+$, **4c**; R = Cy, $E = Bu_4N^+$, **4c′**). The X-ray crystallographic structure of **4a** confirmed the three-legged piano-stool coordination geometry. NMR spectroscopic analysis of compounds **1a, 1a′** and **4a-4c′** unexpectedly revealed complicated spectra, and through subsequent investigations, were attributed to *in situ* monomer-dimer equilibria facilitated by spontaneous chloride ligand dissociation. Complexes **1a** and **1a′** were used as precursors to form formally neutral, zwitterionic complexes $[RuCl(py)(\eta^6\text{-}p\text{-cymene})\{PCy_2(p\text{-}Ph_3BC_6H_4)\}]$, **2** and $[RuCl(MeCN)(\eta^6\text{-}p\text{-cymene})\{PCy_2(p\text{-}Ph_3BC_6H_4)\}]$, **3** via chloride ligand removal using a halide extracting agent.

Acknowledgments

First and foremost, I would like to express my deepest gratitude towards my supervisor, Dr. Greg Spivak. His valuable knowledge, guidance, patience and encouragement throughout my time at Lakehead University allowed me to become a better chemist, educator and person.

I would also like to thank past co-workers Jesse Walker, Mike Beach and Justin Deagle for their support, suggestions and conversations throughout the years. I am truly grateful to have had the opportunity to be part of this great research group.

Finally, I would like to thank the Lakehead University Chemistry Department for their continuous support and friendly atmosphere throughout my studies.

Contents

Abstract.....i

Acknowledgments.....ii

Contents.....iii

List of Figures.....vii

List of Tables.....viii

List of Schemes.....ix

Abbreviations.....xi

1. Introduction.....1

1.1 Anionic Phosphine Ligands.....2

1.1.1 Tridentate Anionic Phosphine Ligands.....2

1.1.1.1 Tris(diphenylphosphinomethyl)phenylborate, $[PhB(CH_2PPh_2)_3]^-$.....3

1.1.1.2 Tri(diisopropylphosphinomethyl)borate, $[PhB(CH_2P^iPr_2)_3]^-$.....4

1.1.2 Bidentate Anionic Phosphine Ligands.....6

1.1.2.1 Bis(phosphino)borate Ligands.....6

1.1.3 Monodentate Anionic Phosphine Ligands.....9

1.1.3.1 Diphenylphosphidoboratabenzene, $[PPh_2(C_5BH_6)]^-$.....10

1.1.3.2 Phosphanylborohydride, $[BH_3PR_2]^-$.....12

1.1.3.3 (Phosphino)tetraphenylborate Ligand, $[PR_2C_6H_4BPh_3]^-$.....14

1.1.4 Summary of Anionic Phosphine Ligands.....15

1.2 Ruthenium-Arene Complexes.....16

1.2.1 Ruthenium-Arene Complexes in Catalysis.....18

1.2.2 Ruthenium-Arene Dimers Bridged by Chloride Ligands.....18

1.2.3 Ruthenium Complexes Exhibiting Monomer-Dimer Equilibria.....19

2. Research Proposal.....22

3. Experimental.....23

3.1 General Considerations.....23

3.2 Synthesis of [PNP][$RuCl_2(\eta^6$-*p*-cymene){PCy_2(*p*-$Ph_3BC_6H_4$)}], **1a**.....24

3.2.1 Synthesis of [Bu_4N][$RuCl_2(\eta^6$-*p*-cymene){PCy_2(*p*-$Ph_3BC_6H_4$)}], **1a'**.....24

3.2.2 Variable Temperature NMR Experiment with Compound **1a'**.....25

3.3 Synthesis of [RuCl(py)(η^6-*p*-cymene){PCy_2(*p*-$Ph_3BC_6H_4$)}], **2**.....25

3.4 Synthesis of [RuCl(MeCN)(η^6-*p*-cymene){PCy_2(*p*-$Ph_3BC_6H_4$)}], **3**.....26

3.5 Synthesis of [PNP][$RuCl_2(\eta^6$-C_6H_6){P^iPr_2(*p*-$Ph_3BC_6H_4$)}], **4a**.....26

3.5.1 Structural Characterization of **4a** via X-ray Crystallography.....27

3.5.2 Synthesis of [Bu_4N][$RuCl_2(\eta^6$-C_6H_6){P^iPr_2(*p*-$Ph_3BC_6H_4$)}], **4a'**.....28

3.5.2.1 Reaction with Compound **4a'** with [Et_4N][Cl].....29

3.5.3 Synthesis of [PNP][$RuCl_2(\eta^6$-C_6H_6){PPh_2(*p*-$Ph_3BC_6H_4$)}], **4b**.....29

3.5.4 Synthesis of [Bu_4N][$RuCl_2(\eta^6$-C_6H_6){PPh_2(*p*-$Ph_3BC_6H_4$)}], **4b'**..... 29

3.5.4.1 Reaction of Compound 4b′ with [Et_4N][Cl].....30

3.5.5 Synthesis of [PNP][$RuCl_2(\eta^6$-C_6H_6){PCy_2(*p*-$Ph_3BC_6H_4$)}], **4c**.....30

3.5.6 Synthesis of [Bu_4N][$RuCl_2(\eta^6$-C_6H_6){PCy_2(*p*-$Ph_3BC_6H_4$)}], **4c'**..... 30

3.6 Synthesis of [$RuCl(\eta^6$-C_6H_6){P^iPr_2(*p*-$Ph_3BC_6H_4$)}]$_2$, **5**.....31

3.6.1 Reaction of Compound **5** with MeCN.....32

3.6.2 Variable Temperature NMR Experiment with Compound **5**.....32

3.7 Attempted Synthesis of

[RuCl(=C=C=CPh$_2$)(η^6-C$_6$H$_6$){P^{i}Pr$_2$(*p*-Ph$_3$BC$_6$H$_4$)}].....32

3.8 Attempted Synthesis of

[RuCl(=C=CHPh)(η^6-C$_6$H$_6$){P^{i}Pr$_2$(*p*-Ph$_3$BC$_6$H$_4$)}].....33

3.9.1 Attemped Synthesis of

[Ru(MeCN)$_2$(η^6-C$_6$H$_6$){P^{i}Pr$_2$(*p*-Ph$_3$BC$_6$H$_4$)}][OTf].....34

3.9.2 Attempted Synthesis of

[Ru(MeCN)$_2$(η^6-C$_6$H$_6$){PPh$_2$(*p*-Ph$_3$BC$_6$H$_4$)}][BF$_4$].....35

3.9.3 Attempted Synthesis of

[Ru(MeCN)$_2$(η^6-C$_6$H$_6$){P^{i}Pr$_2$(*p*-Ph$_3$BC$_6$H$_4$)}][BF$_4$].....36

4. Results and Discussion.....37

4.1 Synthesis and Chemistry Involving [E][RuCl$_2$(η^6-*p*-cymene){PCy$_2$(*p*-Ph$_3$BC$_6$H$_4$)}] (E = PNP, **1a**; Bu$_4$N, **1a′**).....37

4.2 Synthesis of [RuCl(py)(η^6-*p*-cymene){PCy$_2$(*p*-Ph$_3$BC$_6$H$_4$)}] **2** and [RuCl(MeCN)(η^6-*p*-cymene){PCy$_2$(*p*-Ph$_3$BC$_6$H$_4$)}], **3**.....42

4.3 Synthesis and Chemistry of [E][RuCl$_2$(η^6-C$_6$H$_6$){PR$_2$(*p*-Ph$_3$BC$_6$H$_4$)}] (R = ^{i}Pr, R = PNP, **4a**; R = ^{i}Pr, R = Bu$_4$N, **4a′**; R = Ph, R = PNP, **4b**; R = Ph, R = Bu$_4$N, **4b′**; R = Cy, R = PNP, **4c**; R = Cy, R = Bu$_4$N, **4c′**)...46

4.4 NMR Experiment: Compound **4a′** with [Et$_4$N][Cl].....52

4.5 Synthesis and Chemistry of [RuCl(η^6-C$_6$H$_6$){P ^{i}Pr$_2$(*p*-Ph$_3$BC$_6$H$_4$)}]$_2$, **5**...54

4.6 Attempted Synthesis of

[Ru(MeCN)$_2$(η^6-C$_6$H$_6$){P^{i}Pr$_2$(*p*-Ph$_3$BC$_6$H$_4$)}][OTf].....57

4.7 Attempted Synthesis of

$[Ru(MeCN)_2(\eta^6\text{-}C_6H_6)\{PR_2(p\text{-}Ph_3BC_6H_4)\}][BF_4]$.....59

4.8 Attempted Synthesis of

$[RuCl(=C=C=CPh_2)(\eta^6\text{-}C_6H_6)\{P^iPr_2(p\text{-}Ph_3BC_6H_4)\}]$.....61

4.9 Attempted Synthesis of

$[RuCl(=C=CHPh)(\eta^6\text{-}C_6H_6)\{P^iPr_2(p\text{-}Ph_3BC_6H_4)\}]$.....63

5. Conclusion.....65

6. References.....67

List of Figures

Figure 1 Representation of a tridentate anionic phosphine.....2

Figure 2 Representation of the bis(phosphino)borate ligands.....6

Figure 3 Representations of ruthenium half-sandwich complexes.....17

Figure 4 Examples of ruthenium-arene dimers bridged by chloride ligands.....19

Figure 5 $^{31}P\{^{1}H\}$ NMR spectrum of compound **1a'**.....39

Figure 6 ^{1}H NMR spectrum of compound **1a'**.....40

Figure 7 $^{31}P\{^{1}H\}$ NMR spectrum of compound **2**.....44

Figure 8 ^{1}H NMR spectrum for compound **2**.....44

Figure 9 $^{31}P\{^{1}H\}$ NMR spectrum of compound **3**.....45

Figure 10 ^{1}H NMR spectrum for compound **3**.....45

Figure 11 ORTEP Drawing of [PNP][$RuCl_2(\eta^6$-$C_6H_6)\{P^iPr_2(p$-$Ph_3BC_6H_4)\}$], **4a**...50

Figure 12 $^{31}P\{^{1}H\}$ NMR spectrum of Complex **4a'** and **4a'** in the presence of excess chloride ions.....53

Figure 13 Arene region of the ^{1}H NMR spectrum for the η^6-C_6H_6 ligand of complex **4a'** and **4a'** in the presence of excess chloride ions.....54

Figure 14 $^{31}P\{^{1}H\}$ NMR spectrum for compound **5**.....56

Figure 15 ^{1}H NMR spectrum for compound **5**.....57

List of Tables

Table 1 CO stretching frequencies of $LIr(CO)_2$ (L = κ^3- $PhB(CH_2PPh_2)_3$, κ^3- Tp^{Me2}, η^6-Cp*) in hexanes....4

Table 2 CO stretching frequencies of metal-carbonyl compounds containing tridentate phosphines....5

Table 3 CO stretching frequencies of metal-carbonyl compounds containing bidentate phosphines....9

Table 4 CO stretching frequencies of metal-carbonyl compounds containing monodentate phosphines....11

Table 5 Selected bond distances for metal-carbonyl compounds....11

Table 6 Selected bond lengths and bond angles for chalcogenated phosphanylborohydrides and their triorganyl analogues....13

Table 7 Crystal data and structural refinement for **4a**....28

Table 8 Selected bond lengths and bond angles for [PNP][$RuCl_2(\eta^6$-$C_6H_6)\{P^iPr_2(p$-$Ph_3BC_6H_4)\}$], **4a**....51

List of Schemes

Scheme 1 Synthetic strategy for preparing [Li{TMEDA)][PhB(CH_2PPh_2)$_3$]....3

Scheme 2 Synthetic strategy for preparing [Tl][PhB(CH_2PiPr_2)$_3$]....5

Scheme 3 Synthetic scheme for preparing the dimethyldiaryltin reagents....7

Scheme 4 Synthetic scheme for preparing the diarylchloroboranes....8

Scheme 5 Example of the synthetic scheme for preparing a specific lithio phosphine....10

Scheme 6 Synthetic scheme for preparing $CpFe(CO)_2$(DPB)....10

Scheme 7 Synthetic strategy to forming phosphanylborohydrides....12

Scheme 8 Synthetic strategy to forming chalcogenated phosphanylborohydrides...12

Scheme 9 Scheme for preparing (phosphino)tetraphenylborate ligands....15

Scheme 10 Example of the formation of [$RuCl_2(\eta^6$-arene)(L)] (L= PPh_3)....19

Scheme 11 Monomer-dimer equilibrium of [$RuCl(\eta^5$-Cp*)(PMe^iPr_2)]....20

Scheme 12 Monomer-dimer equilibrium for [$RuCl_3(\eta^6$-*p*-cymene)][Ph_4P]....21

Scheme 13 Synthetic strategy to forming compounds **1a** and **1a'**....37

Scheme 14 Proposed monomer-dimer equilibria for Compounds **1a** and **1a'**....41

Scheme 15 Synthetic approach to forming compounds **2** and **3**....43

Scheme 16 Synthetic approach to forming compounds **4a-4c'**....46

Scheme 17 Proposed *in situ* monomer-dimer equilibria for compounds **4a-4c'**....48

Scheme 18 Synthetic approach to forming compound **5**....54

Scheme 19 Example of ruthenium-bis(acetonitrile) complexes serving as precursors to ligand substitution....58

Scheme 20 Proposed synthetic strategy for forming

[Ru(MeCN)$_2$(η^6-C_6H_6){P^iPr_2(*p*-$Ph_3BC_6H_4$)}][OTf].....58

Scheme 21 Proposed synthetic approach to forming

[Ru(MeCN)$_2$(η^6-C_6H_6){PR_2(*p*-$Ph_3BC_6H_4$)}][BF_4].....59

Scheme 22 General method of preparing ruthenium-allenylidenes.....61

Scheme 23 Proposed synthetic strategy for forming

[RuCl(=C=C=CPh_2)(η^6-C_6H_6){PR_2(*p*-$Ph_3BC_6H_4$)}].....62

Scheme 24 Example of forming ruthenium-vinylidenes.....63

Scheme 25 Proposed synthetic strategy for forming

[RuCl(=C=CHPh)(η^6-C_6H_6){P^iPr_2(*p*-$Ph_3BC_6H_4$)}].....64

Abbreviations

δ	chemical shift (ppm)
BDNA	1,8-bis(diphenylphosphinomethyl)naphthalene
Bu	butyl
^{t}Bu	*tert*-butyl
Cp	cyclopentadienyl
Cp*	1,2,3,4,5-pentamethylcyclopentadienyl
Cy	cyclohexyl
°C	degrees Celsius
$^{13}C\{^1H\}$	proton decoupled carbon-13 NMR spetrum
d	doublet
DPB	diphenylphosphidoboratabenzene
dppp	1,3-bis(diphenylphosphino)propane
g	grams
^1H	proton NMR spectrum
Hz	Hertz
J	coupling constant (Hz)
K	absolute temperature (Kelvin)
m	multiplet
Me	methyl
mL	millilitres
mol	moles
NMR	nuclear magnetic resonance

p	*para*
ppm	parts per million
Ph	phenyl
PNP^+	bis(triphenylphosphine)iminium ion
^{i}Pr	isopropyl
$^{31}P\{^{1}H\}$	proton decoupled phosphorus-31 NMR spectrum
ORTEP	Oak Ridge Thermal Ellipsoid Plot program
OTf	trifluoromethanesulfonate
s	singlet
t	triplet
THF	tetrahydrofuran
TMEDA	tetramethylethylenediamine
Tp	hydridotris(pyrazolyl)borate
Tp*	tris(3,5-dimethylpyrazolyl)borate
Triphos	1,1,1-tris(diphenylphosphinomethyl)ethane
VT	variable temperature

1. Introduction

An important element of organometallic chemistry is the drive towards developing compounds for catalytic applications. In recent years, there has been a great deal of emphasis on developing metal-based complexes for industrial applications and for the synthesis of fine chemicals. Specific properties can be incorporated into a complex through certain ligand-metal combinations. A wide variety of ligand classes have been explored, however certain types of ligands have played a more significant role than others in organometallic chemistry. One class of ligands which has received considerable attention in past decades is phosphorus-based ligands. Phosphorus-based ligands, specifically tertiary phosphines, exhibit a wide range of electronic, steric and coordination behaviours, and are still used predominately as co-ligands for transition metal complexes[1]. Tertiary phosphines are particularly important and extensively studied, and novel structural variants have been achieved by altering the substituents on the phosphorus donor atom[1]. Manipulating the substituents of the phosphorus scaffold is essential to developing complexes with unique properties[2]. One particularly unique approach involves incorporating a counteranion within the phosphorus scaffold thus yielding an anionic phosphine, as opposed to the more conventional neutral phosphine. Anionic phosphines have shown great potential in supporting novel complexes, for example, in catalytically active zwitterionic complexes[3]. Charge-neutral zwitterionic complexes supported by anionic phosphines may exhibit increased solubilities in low polarity solvents, limit coordination of solvents and increase tolerance towards substrate functional groups. Catalytically active charge-neutral zwitterionic complexes would eliminate active site competition between the substrate and a counterion, as the

counterion would be buried within the ligand. These advantages highlight the importance of developing anionic phosphine ligands for potential application in organometallic chemistry. A discussion on several sub-classes of anionic phosphines follows.

1.1 Anionic Phosphine Ligands

Several types of anionic phosphines have been developed, with each possessing distinct structural, electronic and coordination properties. Polydentate and monodentate ligand types are known. The following sections detail the synthesis and properties of several anionic phosphine ligands bearing a borate unit, each grouped in their appropriate type.

1.1.1 Tridentate Anionic Phosphine Ligands

Tridentate anionic phosphines donate six-electrons by coordinating through three phosphorus donor atoms in a tripodal fashion (Figure 1)[4,5]. This class of anionic phosphine is potentially isoelectronic with ligands such as cyclopentadiene (Cp) and hydridotris(pyrazolyl)borate (Tp), although Cp and Tp ligands have distinctly different coordination properties[6]. Tridentate anionic phosphine ligands contain soft phosphorus donor atoms, similar to the π-system of Cp ligands, yet coordinate through three σ-donor atoms, similar to Tp ligands. The most common method of synthesis involves using a borate to bridge the phosphorus centres (Figure 1).

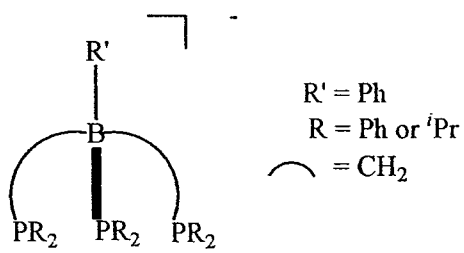

Figure 1: General representation of a tridentate anionic phosphine

1.1.1.1 Tris(diphenylphosphinomethyl)phenylborate, $[PhB(CH_2PPh_2)_3]^-$

The synthesis and characterization of $[PhB(CH_2PPh_2)_3]^-$ was first reported by Barney *et al.* in 1999[4]. Within the phosphine framework, there is a borate bridgehead containing three pendant arms with phosphorus donor atoms at each end. The ligand was prepared by adding dichlorophenylborane to three equivalents of diphenylphosphinomethide to produce the anionic ligand in high yield (Scheme 1).

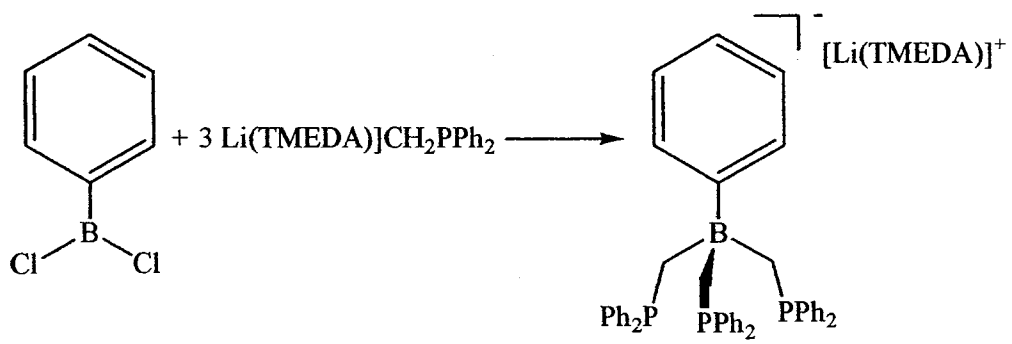

Scheme 1: Synthetic strategy for preparing $[PhB(CH_2PPh_2)_3][Li(TMEDA)]$

There are a number of examples of this phosphine coordinating to a variety of metal-centers[4,7,8]; moreover, the spectroscopic properties of certain complexes has proven beneficial in understanding the electronic properties of the phosphine. For example, one particular study reported the synthesis and characterization of a series of iridium dicarbonyl compounds containing this anionic phosphine, Cp* and Tp* [8]. The stretching frequencies of metal-bound carbonyls allows for a general assessment of the degree of back-bonding and thus the electron richness of the metal, and ultimately suggesting the relative donating ability of the ligand system. Table 1 gives the results for the comparison between the anionic phosphine, Cp* and Tp*.

Table 1: CO stretching frequencies of $LIr(CO)_2$ ($L = \kappa^3$- $PhB(CH_2PPh_2)_3$, κ^3- Tp^*, η^6-Cp*) in hexanes[8]

Complex	(CO), cm^{-1}
$[Tp^*]Ir(CO)_2$	2039, 1960
$Cp^*Ir(CO)_2$	2020, 1953
$[PhB(CH_2PPh_2)_3]Ir(CO)_2$	2024, 1940

Looking at the IR data, the CO stretching frequencies for the Cp* and Tp* analogues were relatively higher in energy when compared to the anionic phosphine, illustrating the electron-richness of the metal-centre for the $[PhB(CH_2PPh_2)_3]Ir(CO)_2$ complex. These observations suggest the electron donating ability of the tridentate anionic phosphine is greater in comparison to Cp* and Tp* derivatives.

1.1.1.2 Tri(diisopropylphosphinomethyl)borate, $[PhB(CH_2P^iPr_2)_3]^-$

Utilizing a similar framework as the $[PhB(CH_2PPh_2)_3]^-$ ligand, J.C. Peters *et al.* prepared an analogous tridentate anionic phosphine, $[PhB(CH_2P^iPr_2)_3]^-$[5]. The synthetic approach to the formation of the phosphine involves the deprotonation of $^iPr_2PMe$ by solid ^{t}BuLi. A stoichiometric amount of TMEDA was added to an ethereal suspension of $^iPr_2PCH_2Li$ to aid in dissolution and subsequent delivery of $PhBCl_2$ to form $[Li(TMEDA)_x][PhB(CH_2P^iPr_2)_3]$. A cation exchange was facilitated by the *in situ* addition of $TlPF_6$ and the ligand was isolated as the thallium salt $[Tl][PhB(CH_2P^iPr_2)_3]$ (Scheme 2).

Substituting the substituents of the phosphine donor atoms with stronger electron releasing groups yields entirely different electronic properties, and also changes the sterics of the phosphine. To illustrate this point, a comparative study was again

performed involving metal carbonyl complexes containing both $[PhB(CH_2PPh_2)_3]^-$ and $[PhB(CH_2P^iPr_2)_3]^-$ ligands (Table 2).

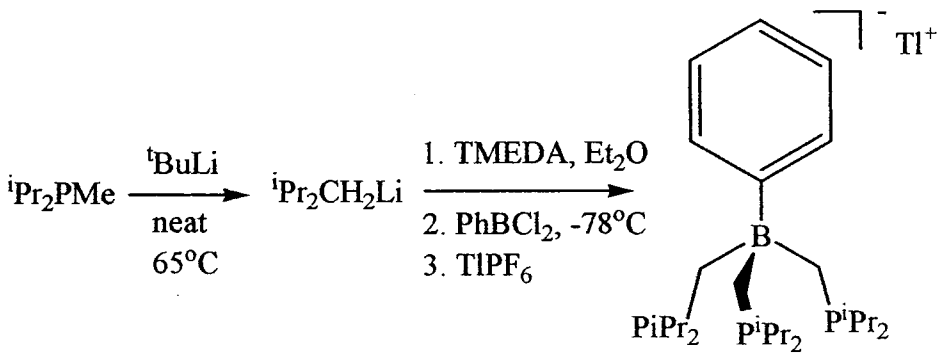

Scheme 2: Synthetic strategy for preparing $[Tl][PhB(CH_2P^iPr_2)_3]$

Table 2: CO stretching frequencies of metal-carbonyl compounds containing tridentate phosphines

Complex	ν(CO), cm^{-1}
$[PhB(CH_2P^iPr_2)_3]FeCl(CO)$[5]	2020[a]
$[PhB(CH_2P^iPr_2)_3]CoCl(CO)$[5]	2010[a]
$[PhB(CH_2PPh_2)_3]CoCl(CO)$[5]	2036[a]
$[PhB(CH_2P^iPr_2)_3]Co(CO)_2$[5]	1990, 1904[a]
$[PhB(CH_2PPh_2)_3]Co(CO)_2$[5]	2008,1932[a]
$Cp^*Co(CO)_2$[9]	2011, 1949[b]
$[Tp^*]Co(CO)_2$[10]	2016, 1939[c]
$CpCo(CO)_2$[11]	2033, 1972[b]
$[(triphos)Co(CO)_2][PF_6]$[12]	2030, 1972[d]

[a]Benzene/KBr. [b]Cyclohexane/KBr. [c]Toluene/KBr. [d]CH_2Cl_2/KBr

A 26 cm^{-1} difference was observed between $[PhB(CH_2PPh_2)_3]Co(CO)Cl$ and $[PhB(CH_2P^iPr_2)_3]Co(CO)Cl$, which indicates the greater electron donating ability of the $[PhB(CH_2P^iPr_2)_3]^-$ ligand. A similar trend is exhibited for dicarbonyl compounds when comparing both anionic phosphines with Cp, Cp* and Tp* derivatives. The reported CO

stretching frequencies illustrate that the electron donating properties of tridentate anionic phosphines can be altered by substituting the substituents on the donor atoms.

1.1.2 Bidentate Anionic Phosphine Ligands

Bidentate anionic phosphines are described as four electron-donating ligands that coordinate through two tethered phosphorus atoms in a chelating fashion. Formally speaking, a borate unit is incorporated into the phosphorus scaffold to provide the desired anionic nature of the phosphine. Similar to tridentate anionic phosphines, the substituents of the phosphorus donor atom can be altered to provide structural variants exhibiting unique electronic, steric and coordination behaviours.

1.1.2.1 Bis(phosphino)borate ligands

This class of bidentate phosphine contains a borate unit within the ligand framework with two ligating phosphine substituents for metal coordination[13-15]. With the borate unit buried within the ligand backbone and relatively isolated from the phosphorus donor atoms, the phosphine ligand exhibits similar structural properties as bis(phosphine) ligands (Figure 2)[13].

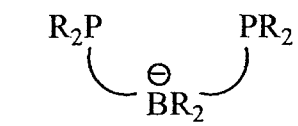

⌒ = CH_2, for example

Figure 2: General representation of the bis(phosphino)borate ligands

The most established method of forming bis(phosphino)borate ligands is via nucleophilic addition to borane compounds, for example, delivering a phosphinoalkyl carbanion to a borane electrophile. A report by J.C. Peters *et al.* describes detailed

methods of synthesizing a variety of bis(phosphino)borate ligands via the borane electrophile method[13]. The first step in the preparation of the ligands is the formation of the borane synthons. Preparation of these synthons requires dimethyldiaryltin reagents. Dimethyldiaryltin compounds are readily formed by reacting dimethyldichlorotin with a specific aryl-Grignard or arylithium reagent to prepare the corresponding dimethyldiaryltin reagent (Scheme 3).

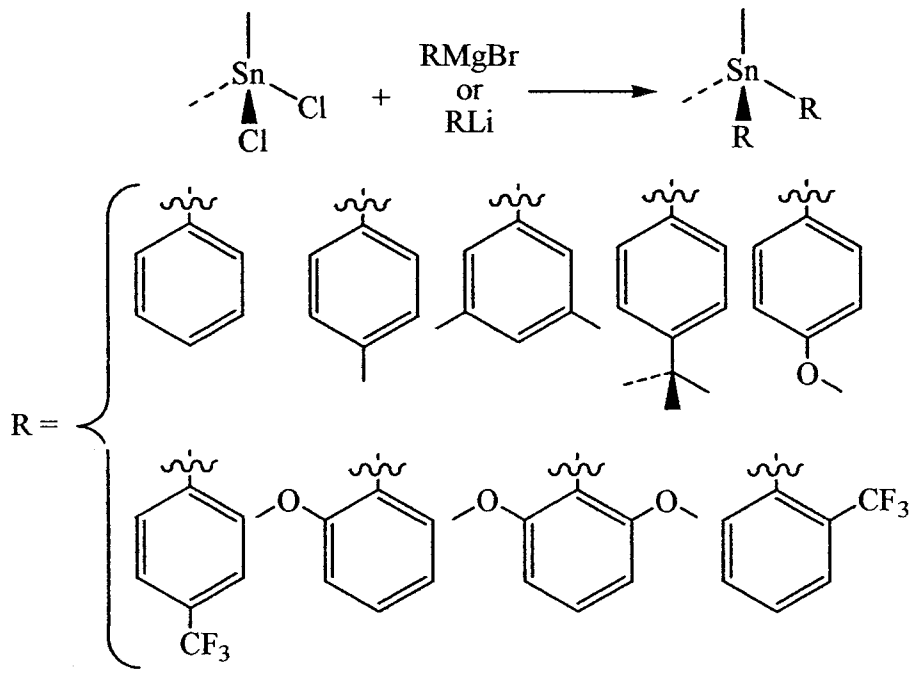

Scheme 3: Synthetic scheme for preparing the dimethyldiaryltin reagents[13]

The dimethyldiaryltin reagent was further reacted with a heptane solution of BCl_3 yielding the desired diarylchloroboranes (Scheme 4).

Similar to tridentate anionic phosphines, the phosphine precursors are prepared by the deprotonation of a dialkylmethyl- or diarylmethylphosphine using an organolithium reagent. The final step of the ligand synthesis involves the condensation of two equivalents of the lithio phosphine reagent with the desired borane synthon[13].

Preparation of each reagent varies depending on the particular borane electrophile and lithiated phosphine.

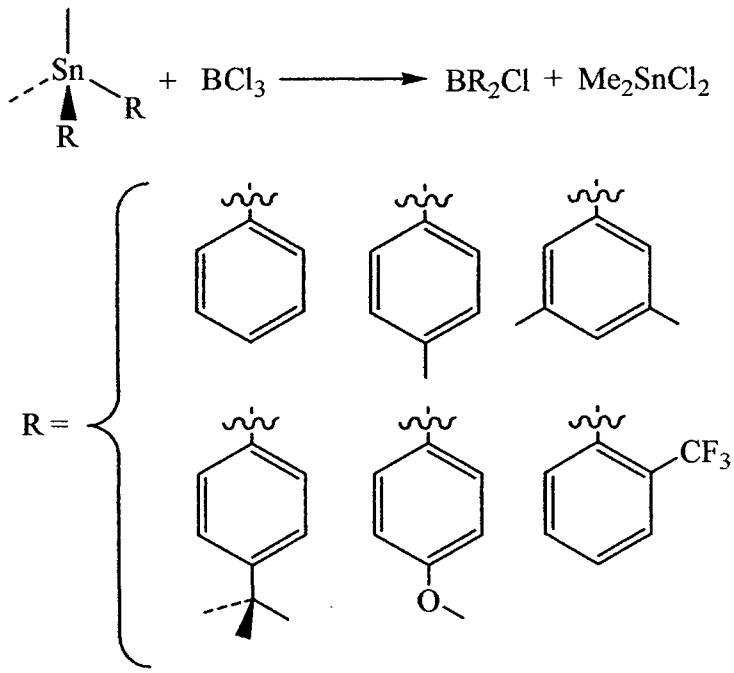

Scheme 4: Synthetic scheme for preparing the diarylchloroboranes[13]

Similar to the tridentate phosphines, the electronic nature of the bis(phosphino)borate ligands were investigated through comparative studies of certain metal-carbonyl derivatives. Looking at the vibrational frequencies of various metal-carbonyl complexes, the bis(phosphino)borate ligands appear to exhibit a greater electron donating ability compared to their neutral counterparts (Table 3).

There is a significant difference when comparing the platinum dppp and ($Ph_2Si(CH_2PPh_2)_2$) complexes with the analogous complex containing the $[Ph_2B(CH_2PPh_2)_2]^-$ ligand. The two cationic complexes have the same ν(CO) value, whereas the neutral complex has a value 24 cm^{-1} lower in energy. The difference in

stretching frequencies may be used to gauge the electron donating ability of the anionic phosphines in comparison to structurally similar neutral analogues.

Table 3: CO stretching frequencies of metal-carbonyl compounds containing bidentate phosphines[13]

Complex	ν(CO), cm^{-1} [a]
$[Ph_2B(CH_2PPh_2)_2]Pt(Me)(CO)$	2094
$[(Ph_2Si(CH_2PPh_2)_2)Pt(Me)(CO)][B(C_6F_5)_4]$	2118
$[(dppp)Pt(Me)(CO)][B(C_6F_5)_4]$	2118
$[Ph_2B(CH_2PPh_2)_2]Mo(CO)_4][ASN]$	2005
$[(Ph_2Si(CH_2PPh_2)_2)Mo(CO)_4]$	2018
$[(dppp)Mo(CO)_4]$	2018

[a] CH_2Cl_2 solution.

A similar trend is observed for the stretching frequencies of the tetracarbonyl molybdenum complexes. The molybdenum complex containing the anionic phosphine had a CO stretch 13 cm^{-1} lower in energy than the dppp and $(Ph_2Si(CH_2PPh_2)_2)$ systems. Once again, this difference in CO stretching frequencies illustrates the relative electron-richness of the metal-centre and the greater electron-donating ability of the anionic phosphine.

1.1.3 Monodentate Anionic Phosphine Ligands

Monodentate anionic phosphines are similar to tridentate and bidentate anionic phosphines, and also contain a borate unit tethered to a substituted tertiary phosphine donor atom. There are many examples of anionic monodentate phosphine analogues having unique structural and electronic properties as a consequence of having altered the substituents on the tertiary phosphine[16-19].

1.1.3.1 Diphenylphosphidoboratabenzene, $[PPh_2(C_5BH_6)]^-$

First reported by G.C. Fu *et al.* in 1996, diphenylphosphidoboratabenzene (DPB) is regarded as an isosteric anionic derivative of triphenylphosphine[16]. The DPB ligand was formed by adding potassium diphenylphosphide to a cooled THF solution of borabenzene-PMe_3 (Scheme 6).

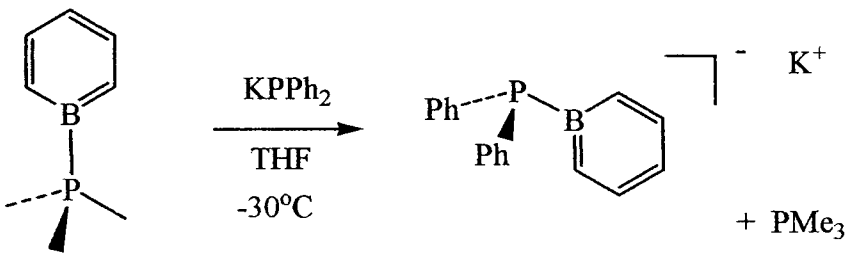

Scheme 5: Synthetic scheme for preparing the DPB ligand[16]

A variety of transition metal complexes containing the DPB ligand were prepared by treating transition metal halides with K-DPB, for example, the addition of K-DPB to $CpFe(CO)_2I$ (Scheme 6).

$$CpFe(CO)_2I + \text{K-DPB} \xrightarrow[-78^\circ C \rightarrow 20^\circ C]{THF} CpFe(CO)_2(DPB)$$

Scheme 6: Synthetic scheme for preparing $CpFe(CO)_2(DPB)$[20]

The synthesis of $CpFe(CO)_2(DPB)$ allowed for the carbonyl vibrations to be compared to those observed for $[CpFe(CO)_2(PPh_3)]^+$ and $CpFe(CO)_2(PPh_2)$. Looking at ν(CO) (Table 4), the DPB ligand possesses significantly greater electron-donating ability when compared to the triphenylphosphine analogue. The complex $CpFe(CO)_2(PPh_2)$ has the lowest carbonyl vibrations indicating a greater electron density about the metal centre,

however the diphenylphoshido ligand has a lone pair of electrons which may contribute to the electron richness of the metal.

Table 4: CO stretching frequencies of metal-carbonyl compounds containing monodentate phosphines

Complex	ν(CO), cm^{-1}
$[CpFe(CO)_2(PPh_3)]Cl \cdot 3H_2O$[21]	2025, 2070[a]
$CpFe(CO)_2(DPB)$[20]	1982, 2024[b] 1989, 2035[c]
$CpFe(CO)_2(PPh_2)$[22]	1966, 2015[d]

[a]Nujol. [b]KBr. [c]CH_2Cl_2 solution. [d]Cyclohexane solution

Single crystal X-ray structures were determined in order that structural comparisons between $[CpFe(CO)_2(PPh_3)]Cl \cdot 3H_2O$ and $CpFe(CO)_2(DPB)$ could be made (Table 5).

Table 5: Selected bond distances for metal-carbonyl compounds

Complex	Fe-(CO) (Å)	C-O (Å)
$[CpFe(CO)_2(PPh_3)]Cl \cdot 3H_2O$[21]	1.767(4) 1.775(4)	1.138(5) 1.140(5)
$CpFe(CO)_2(DPB)$[20]	1.741(10) 1.743(10)	1.170(10) 1.167(10)

Interestingly, the Fe-CO bond distances between the two complexes differ. The distances between the metal and CO ligands for $CpFe(CO)_2(DPB)$ were shorter than the bond distances for $[CpFe(CO)_2(PPh_3)]Cl \cdot 3H_2O$. This trend can be associated with the greater electron donating ability of the anionic phosphines. A greater degree of back-bonding increases the metal-ligand bond order resulting in a shorter metal-ligand bond. In addition to the Fe-CO bond distances, the C-O bond distances between the two complexes are quite different. The C-O bond distance for $CpFe(CO)_2(DPB)$ were longer

than the bond distances for $[CpFe(CO)_2(PPh_3)]Cl \cdot 3H_2O$. Once again, the difference in the bond distances is likely a function of the greater electron donating ability of the anionic phosphine. A greater degree of back-bonding between the metal orbital and the π^* orbital on the CO ligand causes the bond order of the CO ligand to decrease resulting in a longer C-O bond.

1.1.3.2 Phosphanylborohydride, $[BH_3PR_2]^-$

This class of anionic ligands may be regarded as diorganophosphanes with a BH_3 substituent. A recent report by Dornhaus *et al.* describes the synthetic strategy of preparing these anionic ligands[17]. The phosphanylborohydrides are formed by the deprotonation of a phosphane-borane adduct with potassium hydride (Scheme 7).

$$HPR_2BH_3 + KH \longrightarrow K[PR_2BH_3]$$

$R = Ph, {}^tBu$

Scheme 7: Synthetic strategy to forming phosphanylborohydrides[17]

A series of chalcogenated phosphanylborohydrides were prepared to investigate the influence that BH_3 has on the electronic distribution of the compounds. The chalcogenated phosphanylborohydrides were prepared by treating $K[PR_2BH_3]$ with a corresponding chalcogen (Scheme 8).

$$K[PR_2BH_3] + N_2O \longrightarrow K[OPR_2BH_3]$$

$$K[PR_2BH_3] + E \longrightarrow K[EPR_2BH_3]$$

$R = Ph, {}^tBu$

$E = S, Se, Te$

Scheme 8: Synthetic strategy to forming chalcogenated phosphanylborohydrides

X-ray crystallography and NMR spectroscopy were the two methods used for the characterization of the compounds. Selected bond lengths and bond angles were compared between the anionic and neutral phosphanes (Table 6).

Table 6: Selected bond lengths and bond angles for chalcogenated phosphanylborohydrides and their triorganyl analogues

Compound	P-E (Å) (E = O, S, Se, Te)	Average P-C_i (Å)	C-P-C (°)
$[K(18\text{-c-}6)][OPPh_2BH_3]$[18]	1.514(1)	1.832(1)	100.4(1)
$OPPh_2CH_3$[18]	1.494(2)	1.808(3)	105.1(1)
$[K(18\text{-c-}6)][SPPh_2BH_3]$[18]	1.987(4)	1.822(9)	101.9(4)
$SPPh_3$[23]	1.950(3)	1.817(8)	105.7(6)
$[K(18\text{-c-}6)][SePPh_2BH_3]$[18]	2.182(1)	1.828(2)	102.3(1)
$SePPh_3$[24]	2.106(1)	1.826(10)	105.7(7)

An interesting trend is observed for the C-P-C bond angles. All complexes containing the phosphanylborohydrides have a smaller C-P-C bond angle when compared to their neutral analogues. It is often observed that four coordinate atoms with strong electronegative substituents exhibit greater *p* character, resulting in smaller bond angles[25]. The differences in the bond angles among the phosphine analogues may be attributed to this trend. The P-C bond lengths for the anionic compounds are longer than the neutral analogues, which support greater *p* character for the phosphanylborohydride ligands.

NMR spectroscopy was used to determine the coupling constants for the chalcogenated phosphanylborohydrides. The $^1J_{PX}$ coupling constants (X = B, C, Se, Te) allows for the degree of *s* character in the P-X bonds to be investigated. The coupling constants for P-B($^1J_{PB}$), P-CH_3($^1J_{PC}$) and P-C(ipso carbon of phenyl, $^1J_{PCi}$) all increase when the calcogeno substituent attaches to the phosphorus centres of $K(PPh_2BH_3)$, $K(P^tBu_2BH_3)$ and PPh_2CH_3, respectively. The NMR spectroscopic data suggests that

$[PR_2BH_3]^-$ exhibits greater *p* character towards the corresponding chalcogen atom. These findings, along with structural data, indicate a stronger E-P interaction with $[PR_2BH_3]^-$ than with PPh_2CH_3. If the E-P bond is stronger with $[PR_2BH_3]^-$, likely will be stronger for L_nM also. As a result, the phosphanylborohydride ligands appear to be better donors compared to their neutral analogues.

1.1.3.3 (Phosphino)tetraphenylborate Ligand, $[PR_2C_6H_4BPh_3]^-$

These anionic phosphine ligands were constructed using techniques similar to those used for the previously reported anionic phosphines discussed in sections 1.1.1.2 and 1.1.2.1. Incorporating an anionic borate unit within the ligand framework, the (phosphino)tetraphenylborate ligands are regarded as a monodentate tertiary phosphine containing a tetraphenylborate anion. First reported by J.C. Peters[19], the synthetic strategy for the preparation of the (phosphino)tetraphenylborate ligands include the addition of triphenylborane to preformed lithio arylphosphines at low temperatures (Scheme 9). The arylphosphines were generated by the lithiation of either the *para*- or *meta*- substituted bromoarylphosphines. A variety of ligands were prepared by altering the bromoarylphosphine substituents.

The stability and coordination chemistry of these phosphines were briefly reported. In general, these phosphines are stable towards oxidation and hydrolysis over a period of two weeks under an atmosphere of air in an acetone solution. The synthesis of $[^nBu_4N][Mo(CO)_5(P^{meta\text{-}i}Pr_2C_6H_4BPh_3)]$ allowed for a comparison with a neutral analogue $Mo(CO)_5[P^{meta\text{-}i}Pr_2C_6H_4SiPh_3]$ via IR spectroscopy. The CO stretching frequencies for $[^nBu_4N]\{Mo(CO)_5[P^{meta\text{-}i}Pr_2C_6H_4BPh_3]\}$ and $Mo(CO)_5[P^{meta\text{-}i}Pr_2C_6H_4SiPh_3]$ were determined to be 2070, 1942 cm^{-1} and 2065, 1925 cm^{-1}, respectively[19]. The CO stretches

observed for the anionic carbonyl complex are lower in energy compared to the neutral complex. These differences may be attributed to higher electron richness of the metal centre due to the greater electron-donating ability of the anionic phosphine.

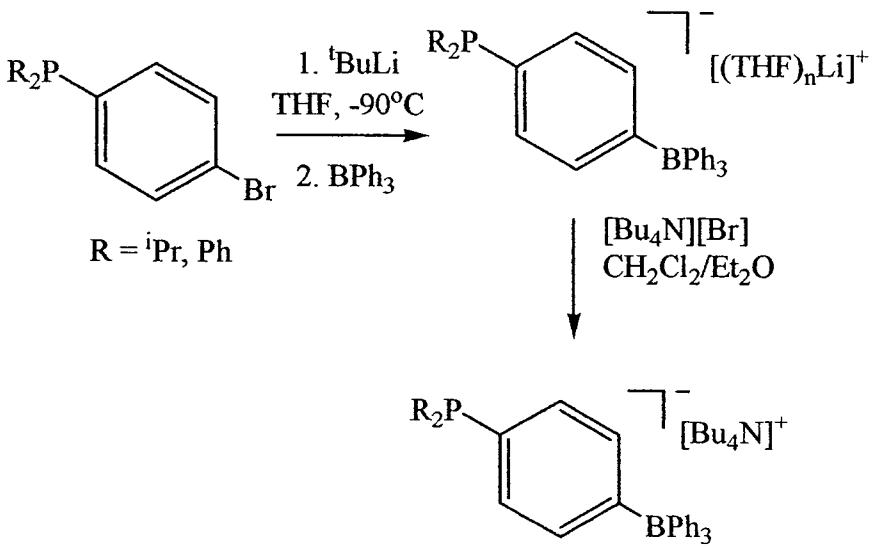

Scheme 9: Scheme for preparing (phosphino)tetraphenylborate ligands[19]

1.1.4 Summary of Anionic Phosphine Ligands

There are a number of selected themes among the anionic phosphine ligands detailed above. Each phosphine has a borate counteranion incorporated within the phosphine scaffold to define the structural variants. In most cases, the anionic phosphines were used as co-ligands in a variety of metal complexes. Many of these metal complexes were used to investigate the coordination properties of the anionic phosphine ligands, for example, metal carbonyls. The spectroscopic and structural data of the complexes suggest each class of anionic phosphine ligand may have enhanced electron-donating abilities, when compared to their neutral counterparts. These anionic phosphine ligands, therefore, show great potential as co-ligands for metal complexes in catalysis. In fact, there are a number of examples of metal complexes exhibiting catalytic

activity while bearing an anionic phosphine ligand[3]. These charge-neutral zwitterionic complexes are known to promote organic transformations, including copolymerization of CO and ethylene[3a], C-H bond activation of amines[3c] and hydrogenolysis[3d], thus illustrating a potential application of anionic phosphine ligands in organometallic chemistry.

1.2 Ruthenium-Arene Complexes

Advances in the field of transition metal chemistry have been paced by the catalytic activity of many complexes in organic synthesis. One transition metal which has garnered much attention in recent years is ruthenium because of its high catalytic reactivity and diverse range of coordination geometries[26]. The structural and electronic properties of metal complexes can be tailored by altering the ligands of the complex. Facially bound arene ligands play a prominent role in ruthenium chemistry as co-ligands in many catalytically active ruthenium complexes[27].

Facially bound arene ligands have shown tremendous potential as co-ligands due to their relative size, stability and binding affinity to the ruthenium atom. Arene ligands typically coordinate in an η^6-fashion, thus occupying three coordination sites on the metal centre, and producing a monometallic half-sandwich complex[27]. There are numerous other types of ligands that produce half-sandwich complexes such as cyclopentadiene and hydridotris(pyrazolyl)borate derivatives[28] (Figure 3). The general method of forming ruthenium-arene complexes involves a dehydrogenation of the appropriate substrate with ethanolic ruthenium(III) trichloride[29]. For example, refluxing hydrated ruthenium trichloride in ethanol with either 1,3- or 1,4-cyclohexadiene forms $[RuCl_2(\eta^6\text{-}C_6H_6)]_2$[29].

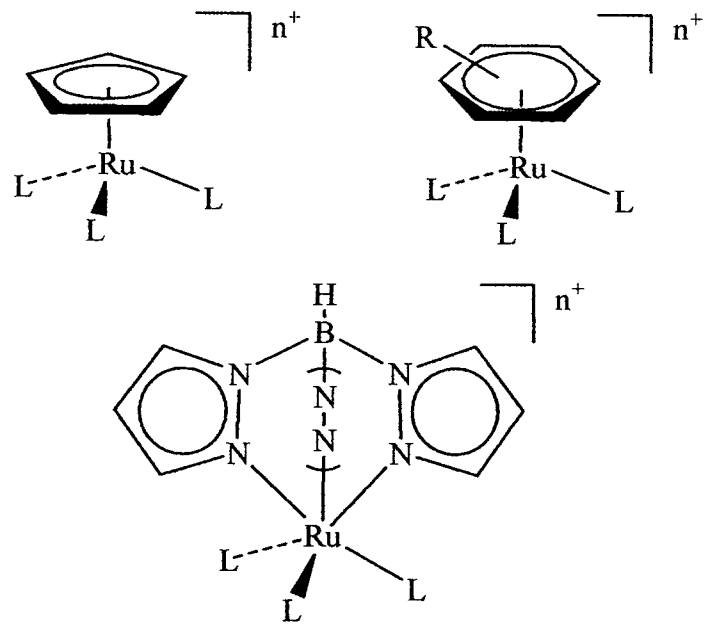

Figure 3: Representations of ruthenium half-sandwich complexes

This approach is quite versatile and is limited only by the availability of the cyclohexadiene precursor. In fact, a wide range of dimeric $[RuCl_2(\eta^6\text{-arene})]_2$ complexes have been prepared using this approach. Arene ligands such as 4-isopropyltoluene (also known as *p*-cymene), toluene and hexamethylbenzene have all proven to be synthetically useful arene ligands in ruthenium chemistry. Interestingly, the arene ligand is generally tightly bound to the ruthenium centre in $[RuCl_2(\eta^6\text{-arene})]_2$, and often requires forcing conditions (i.e., thermal or photochemical) in order for it to be displaced. *p*-Cymene is one of the easier arenes to undergo substitution, although it is unclear why. Perhaps it is related to the substituents on the arene, which increase the steric bulk of the ligand, thus facilitating its substitution.

Arene ligands themselves can undergo unique reactions typically unobserved for the uncoordinated ligand. For example, arene ligands coordinated to a chromium tricarbonyl group become electron deficient and consequently undergo nucleophilic

addition reactions[30]. This is in contrast to the electrophilic substitution reactions typically observed for free aromatics.

1.2.1 Ruthenium-Arene Complexes in Catalysis

The development of ruthenium-arene chemistry is a result of, at least in part, their importance in a variety of catalytic applications. There are numerous examples of ruthenium arene complexes exhibiting excellent catalytic activity in a diverse range of organic transformations, such as hydrogenation reactions, cycloaddition reactions, ring closing metathesis, metathesis polymerization and hydration of terminal alkynes, to name a few[31,32]. The formation of the catalytically active species can proceed in one of two ways. The first requirs partial or full dissociation of the arene ligand, thus forming a coordinatively unsaturated complex[32]. For example, a recent report by O'Connor *et al.* describes enediyne cycloaromatization via ruthenium complexes, and the catalytic system involves *in situ* metal-arene dissociation[33]. The second mechanism involves the formation of a catalytically active species via dissociation of other ligands instead of the arene ligand[31,32]. For example, ruthenium-arene diphosphine complexes are known to promote the hydrogenation of alkenes while retaining the arene ligand[32a,b].

1.2.2 Ruthenium-Arene Dimers Bridged by Chloride Ligands

Halide ligands, in particular chloride, are a common component to many ruthenium-arene complexes and can be found in a variety of coordinating motifs. Most often, chloride ligands are terminally bound. However, the remaining lone pairs of the chloride ligand may also participate in additional bonding interactions, usually with other metals. As alluded to in Section 1.2, there are numerous examples of dimeric ruthenium-arene complexes being bridged by one or two chloride ligands (Figure 4)[29, 35-38].

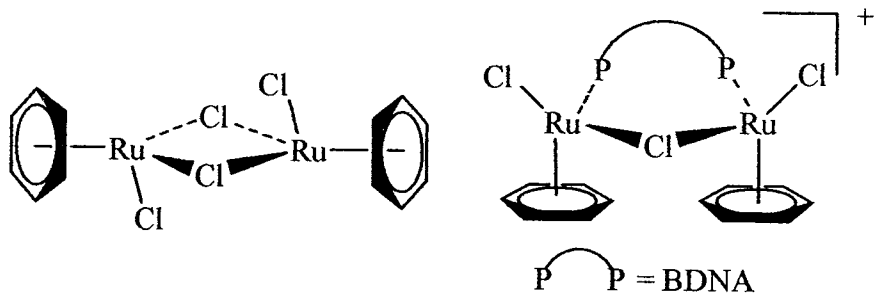

Figure 4: Examples of ruthenium-arene dimers bridged by chloride ligands

Many ruthenium-arene complexes serve as useful precursors to other complexes. For example, the chloride bridge can be cleaved in the presence of a ligand to form monometallic $[RuCl_2(\eta^6\text{-arene})(L)]$ adducts[29,39] starting from the useful precursor $[RuCl_2(\eta^6\text{-arene})]_2$ (Scheme 10). The range of ligands able to cleave the ruthenium-arene dimer is large, however, phosphines play a prominent role in this capacity[29].

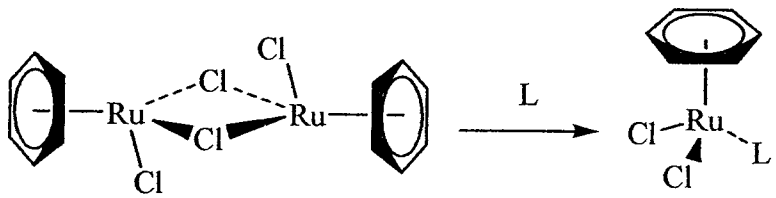

Scheme 10: Example of the formation of $[RuCl_2(\eta^6\text{-arene})(L)]$

1.2.3 Ruthenium Complexes Exhibiting Monomer-Dimer Equilibria

There are a few examples of ruthenium half-sandwich complexes forming *in situ* monomer-dimer equilibria[40,41]. A recent report by Dyson *et al.* details the formation of a ruthenium-arene monomer-dimer equilibrium facilitated by chloride addition and dissociation[40]. The report describes the reaction of $[RuCl_2(\eta^6\text{-}p\text{-cymene})]_2$ with two equivalents of $[Ph_4P][Cl]$ to produce equilibrium amounts of $[Ph_4P][RuCl_3(\eta^6\text{-}p\text{-cymene})]$. Characterization via NMR spectroscopy revealed an *in situ* dynamic equilibrium. The ^1H NMR spectrum for a sample dissolved in CD_2Cl_2 revealed a 1:1

ratio of product:$[RuCl_2(\eta^6\text{-}p\text{-cymene})]_2$; in $CDCl_3$, a 12:1 ratio of product to starting material was observed, suggesting the equilibrium is solvent dependant (Scheme 11).

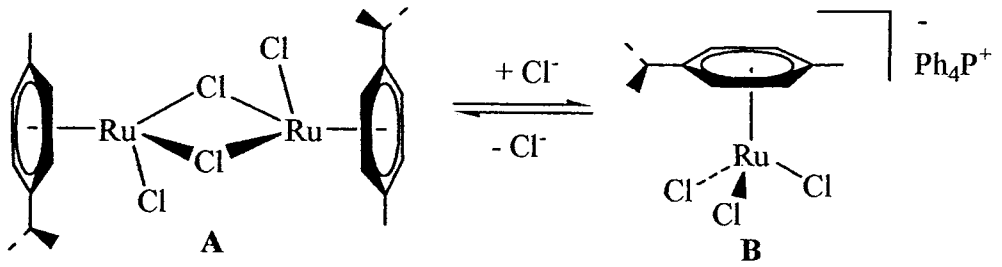

Scheme 11: Monomer-Dimer Equilibrium for $[Ph_4P][RuCl_3(\eta^6\text{-}p\text{-cymene})]$[40]

In the presence of excess $[Ph_4P][Cl]$, the ^1H NMR spectrum indicates an almost complete conversion of $[RuCl_2(\eta^6\text{-}p\text{-cymene})]_2$ (**A**) to $[Ph_4P][RuCl_3(\eta^6\text{-}p\text{-cymene})]$ (**B**). Based on the ^1H NMR data, it is clear that the equilibrium is sensitive to chloride concentration. It is interesting to note that spontaneous chloride dissociation is not observed in $[RuCl_2(PR_3)(\eta^6\text{-}p\text{-cymene})]$, but it is observed in $[RuCl_3(\eta^6\text{-}p\text{-cymene})]^-$. Perhaps the anionic nature of the latter class of compounds promotes halide dissociation. Similar observations were noted for reactions between $[RuCl_2(\eta^6\text{-}p\text{-cymene})]_2$ and [(dibenzo-18-crown-6)K][Cl].

A report by Puerta *et al.* in 2000 describes the formation of a monomer-dimer equilibrium being facilitated by chloride bridging[41]. Although it does not involve a ruthenium-arene complex, it illustrates unsaturated ruthenium half-sandwich complexes involved in monomer-dimer equilibria. Detailed within the report is the synthesis and characterization of the coordinatively unsaturated ruthenium-Cp* complex $[RuCl(\eta^5\text{-}Cp^*)(PMe^iPr_2)]$. The behaviour of the complex in solution was examined via VT NMR spectroscopy and the proposed formula was confirmed through elemental analysis. Within the $^{31}P\{^1H\}$ NMR spectrum, a sharp singlet at $\delta = 31.7$ ppm is observed at room

termpature, and corresponds to the coordinatively unsaturated species. This particular observation is typical for a complex containing a single phosphorus ligand. However, when the temperature is lowered to 180 K, there is a significant change in the $^{31}P\{^{1}H\}$ spectrum. The initial signal corresponding to the unsaturated species broadens and shifts to $\delta = 32.6$ ppm, and a new signal appears at $\delta = 33.4$ ppm. Raising the temperature back to room temperature restores the original NMR spectrum observed for the unsaturated species. This temperature dependant behavior was attributed to a monomer-dimer equilibrium with the signal at $\delta = 33.4$ ppm corresponding to the dimeric species (Scheme 12). Higher temperatures favour the formation of the monomeric species, whereas lower temperatures shift the equilibrium towards the formation of the dimeric species resulting in a mixture of products.

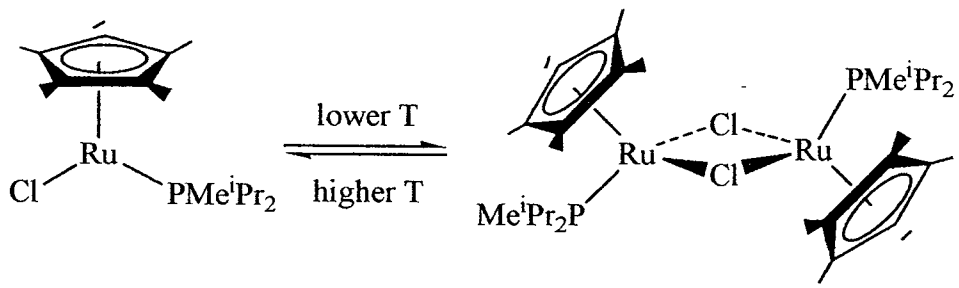

Scheme 12: Monomer-Dimer Equilibrium of [RuCl(η^5-Cp*)(PMe^{i}Pr$_2$)][41]

2. Research Proposal

Phosphorus-based ligands continue to play a vital role as co-ligands in transition metal chemistry. There is still a great deal of interest in developing phosphine ligands with unique structural, electronic and coordination properties. As highlighted in the Introduction, an area of phosphine chemistry which has garnered much attention in recent years is the development of anionic phosphine ligands, including monodentate anionic tertiary phosphines.

Although they possess unique electronic and structural properties, there are few studies focusing on the coordination chemistry of the (phosphino)tetraphenylborate class of ligands, particularly for ruthenium. This provided an opportunity to investigate this novel class of anionic phosphines within the context of catalytically important ruthenium-arene chemistry. There were a number of goals set at the beginning of the project:

1. Develop and implement synthetic strategies which would allow the preparation and isolation of ruthenium-arene complexes bearing this unique class of ligand.
2. Study the structural and electronic properties of the new compounds, and where possible, compare them with their neutral counterparts.
3. Explore any unique chemical reactivity patterns which may arise as a result of coordinating the (phosphino)tetraphenylborate ligand to the metal.
4. Explore the potential development of charge neutral zwitterionic complexes.

3. Experimental

3.1 General Considerations

Experiments described within this section were conducted under an inert atmosphere of prepurified N_2 using standard Schlenk techniques. Acetonitrile, pyridine and methanol were each stored over activated 4A molecular sieves in a bulb fitted with a Teflon tap, and purged with N_2 before use. All other bulk solvents used in large-scale preparations were pre-dried over activated 4A molecular sieves, passed through a column of alumina, purged with N_2 and stored over 4A molecular sieves in bulbs fitted with Teflon taps. NMR solvents were dried with the appropriate drying agents ($CDCl_3$: $CaCl_2$; CD_2Cl_2: CaH_2; C_6D_6: Na metal), vacuum distilled, freeze-pump-thaw degassed three times and stored in round-bottom bulbs with Teflon taps. NMR spectra (^1H, $^{31}P\{^1H\}$, ^{13}C and $^{19}F\{^1H\}$) were obtained using a Varian Unity INOVA 500 MHz spectrometer, with chemical shifts (in ppm) referenced to residual protio solvent peaks (^1H), TMS (^{13}C), external CF_3COOH (^{19}F) or external 85% H_3PO_4 (^{31}P). Elemental analyses were performed on a CEC 240XA analyzer by the Lakehead University Instrumentation Laboratory. Precursors $[RuCl_2(\eta^6\text{-}p\text{-cymene})]_2$[29, 42], $[RuCl_2(\eta^6\text{-}C_6H_6)]_2$[29], $[Ru(MeCN)_3(\eta^6\text{-}C_6H_6)][BF_4]$[29], $[E][PR_2(p\text{-}Ph_3BC_6H_4)]$ (E = Bu_4N^+ or PNP^+, R = Ph or ^iPr)[19] and $[E][PCy_2(p\text{-}Ph_3BC_6H_4)]$ (E = Bu_4N^+ or PNP^+)[43] were prepared according to the literature procedures; the ligands were recrystallized from THF/hexanes. All solid and liquid reagents were purchased from Aldrich or Strem and stored in appropriate environments to preserve product quality and purity.

3.2 Synthesis of [PNP][$RuCl_2(\eta^6$-*p*-cymene){PCy_2(*p*-$Ph_3BC_6H_4$)}], 1a

A Schlenk tube was charged with [$RuCl_2(\eta^6$-*p*-cymene)]$_2$ (0.180 g, 0.293 mmol) and [PNP][PCy_2(*p*-$Ph_3BC_6H_4$)] (0.619 g, 0.611 mmol). Next, CH_2Cl_2 (10 mL) was added via syringe and the deep, dark red solution was allowed to stir for 1.5 hours. After this time, the volatiles were removed under reduced pressure to yield an orange-red product, which was recrystallized from CH_2Cl_2/hexanes via slow diffusion. A methanol wash yielded an analytically pure product. Yield: 77%. Anal. Calc. for $C_{82}H_{85}BCl_2NP_3Ru$: C, 72.24; H, 6.24; N, 1.03. Found: C, 71.98; H, 6.75; N, 0.94%. ^{1}H NMR (499.9 MHz, $CDCl_3$, 22°C): 7.61-6.85 (m, 49H, Ph and PC_6H_4B), 5.05-4.81 (m, 4H *p*-cymene), 3.49 (d, 1H, Cy of phosphine), 2.75 (septet, 1H, ^{i}Pr of *p*-cymene), 2.10-1.16 (m, 38H, Cy of phosphine), 1.84 (s, 3H, Me of *p*-cymene), 1.79 (s, 3H, Me of *p*-cymene), 1.77 (s, 3H, Me of *p*-cymene), 1.06 (d, 6H, ^{i}Pr of *p*-cymene). ^{31}P{^{1}H} (202.3 MHz, $CDCl_3$, 22°C): 22.1 (s, PNP^+), 21.9, 20.5, 19.1 (~6:4:1, all s, PCy_2).

3.2.1 Synthesis of [Bu_4N][$RuCl_2(\eta^6$-*p*-cymene){PCy_2(*p*-$Ph_3BC_6H_4$)}], 1a′

Complex **1a′** was prepared in a manner analogous to that described for the synthesis of **1a** except using [Bu_4N][PCy_2(*p*-$Ph_3BC_6H_4$)]. Product crystallized as a trimethanol solvate (verified by ^{1}H NMR spectroscopy) Yield: 92%. Anal. Calc. for $C_{62}H_{91}BCl_2NPRu$•3MeOH: C. 66.95; H, 8.84; N, 1.20. Found: C, 66.32; H, 8.03; N, 1.02%. ^{1}H NMR (499.9 MHz, $CDCl_3$, 22°C): 7.43-6.93 (m, 19H Ph and PC_6H_4B), 5.09-4.84 (m, 4H, *p*-cymene), 3.49 (d, 1H, Cy of phosphine), 2.84 (septet, 1H, ^{i}Pr of *p*-cymene), 2.69 (m, 8H, Bu), 2.58 (m, 1H, ^{i}Pr of *p*-cymene), 2.14-1.24 (m, 38H, Bu and Cy of phosphine), 1.81 (s, 3H, Me of *p*-cymene), 1.76 (s, 3H, Me of *p*-cymene), 1.74 (s,

3H, Me of *p*-cymene), 1.09 (br d, 6H, ^{i}Pr of *p*-cymene), 0.99 (t, 12H, Bu). $^{31}P\{^{1}H\}$ (202.3 MHz, $CDCl_3$, 22°C): 21.4, 19.9, 18.6 (~1.5:2.5:1, all s, PCy_2).

3.2.2 Variable Temperature NMR Experiment with Compound 1a'

A sample of compound **1a'** (0.020 g, 0.019 mmol) was dissolved in $C_2D_4Cl_2$ (0.5 mL) in a 5 mm NMR tube fitted with a rubber septum attached to an N_2 line. An initial $^{31}P\{^{1}H\}$ spectrum was acquired at 20°C and the temperature was gradually increased to obtain spectra at 40°C, 60 °C and 80°C, respectively. No visible change occured in the shifts or intensity of the $^{31}P\{^{1}H\}$ signals.

3.3 Synthesis of [RuCl(py)(η^6-*p*-cymene){PCy_2(*p*-$Ph_3BC_6H_4$)}], 2

In a Schlenk tube, complex **1a** (0.230 g, 0.169 mmol) was dissolved in CH_2Cl_2 (10 mL). Next, excess pyridine (1.7 mL, 20.5 mmol) was added via syringe, followed by a slight excess of $AgNO_3$ (0.043 g, 0.253 mmol). An orange mixture was produced almost immediately and the mixture was allowed to stir for a total of 2.5 hours. After this time, a yellow solution was obtained and deposited a white precipitate of AgCl. The solution was then filtered through a short plug of silica gel (~2 cm × 1 cm), followed by the removal of the volatiles under reduced pressure to yield a bright yellow solid. Yield: 20.5%. Anal. Calc. for $C_{51}H_{60}BClNPRu$: C, 70.34; H, 6.89; N, 1.61. Found: C, 69.79; H, 6.79; N, 1.14%. ^{1}H NMR (499.9 MHz, $CDCl_3$, 22°C): 8.86 (br, 2H, *o*-H of py), 7.88-6.97 (m, 22H, py, Ph and PC_6H_4B), 5.33, 5.22, 5.04, 4.96 (each m, each 1H, *p*-cymene), 2.44 (septet, 1H, ^{i}Pr of *p*-cymene), 1.38 (s, 3H, Me of *p*-cymene), 1.17 (d, 3H, ^{i}Pr of *p*-cymene), 1.16 (d, 3H, ^{i}Pr of *p*-cymene), 2.26-1.08 (m, 22H, Cy of phosphine). $^{31}P\{^{1}H\}$ (202.3 MHz, $CDCl_3$, 22°C): 27.51 (s, PCy_2).

3.4 Synthesis of [RuCl(MeCN)(η^6-*p*-cymene){PCy_2(*p*-$Ph_3BC_6H_4$)}], 3

In a Schlenk tube, complex **1a** (0.210 g, 0.154 mmol) was dissolved in MeCN (5 mL) via syringe, followed by the addition of a slight excess of $AgNO_3$ (0.032 g, 0.187 mmol). A yellow mixture was produced almost immediately and deposited a white precipitate of AgCl, and the solution was allowed to stir for a total of 2.5 hours. At this time, the solution was then filtered through a short plug of silica gel (~2 cm × 1 cm), followed by the removal of the volatiles under reduced pressure to yield a bright yellow solid. Yield: 30%. Anal. Calc. for $C_{48}H_{58}BClNPRu$: C, 69.67; H, 7.08; N, 1.69%. Found: C, 69.67; H, 7.01; N, 1.39%. ^{1}H NMR (499.9 MHz, $CDCl_3$, 22°C): 7.70-6.98 (m, 19H, Ph and PC_6H_4B), 5.41, 5.60, 5.00, 4.82 (each m, each 1H, cymene), 2.69 (septet, 1H, ^{i}Pr of cymene), 1.84 (s, 3H, Me of cymene), 1.54 (s, 3H, MeCN), 1.14 (d, 3H, ^{i}Pr of cymene), 1.09 (d, 3H, ^{i}Pr of cymene) 2.34-0.88 (m, 22H, Cy of phosphine). ^{31}P{^{1}H} (202.3 MHz, $CDCl_3$, 22°C): 29.72 (s, *P*Cy_2).

3.5 Synthesis of [PNP][$RuCl_2$(η^6-C_6H_6){P^iPr_2(*p*-$Ph_3BC_6H_4$)}] , 4a

A Schlenk tube was charged with [$RuCl_2$(η^6-C_6H_6)]$_2$ (0.100 g, 0.200 mmol) and [PNP][P^iPr_2(*p*-$Ph_3BC_6H_4$)] (0.389 g, 0.400 mmol). Next, CH_2Cl_2 (10 mL) was added via syringe and the deep, dark brown solution was allowed to stir for 2 hours. After this time, the volatiles were removed under reduced pressure to yield a light brown product, which was recrystallized from CH_2Cl_2/hexanes via slow diffusion. Yield: 85%. Despite numerous attempts, analytically pure **4a** could not be obtained. ^{1}H NMR (499.9 MHz, $CDCl_3$, 22°C): 7.62-6.88 (m, 49H, Ph and PC_6H_4B), 5.22-5.19 (m, 6H, C_6H_6), 3.07 (m, 1H, ^{i}Pr of phosphine), 2.78 (m, 1H, ^{i}Pr of phosphine), 1.38 (m, 6H, ^{i}Pr of phosphine) 1.26

(m, 6H, ^{i}Pr of phosphine). $^{31}P\{^{1}H\}$ (202.3 MHz, $CDCl_3$, 22°C): 22.2 (s, PNP^+), 34.3, 33.8, 33.3 (~6:1.5:1, all s, $P^{i}Pr_2$).

3.5.1 Structural Characterization of 4a via X-ray Crystallography

Crystals of compound **4a** were grown by slow diffusion of hexanes into a concentrated CH_2Cl_2 solution over several days at room temperature. The crystals were mounted on a glass fibre with grease and cooled to -93°C in a stream of nitrogen gas using a Cryostream Controller 700. Diffraction data was collected using a Bruker SMART APEX II X-ray diffractometer with graphite-monochromated MoKα radiation (λ = 0.71073 Å), operating at 50 kV and 30 mA over 2θ ranges of 4.20 ~ 52.00°. No significant decay was observed during the data collection. Data were processed on a PC using the Bruker AXS Crystal Structure Analysis Package[44]: Data collection: APEX2 (Bruker, 2006); cell refinement: SAINT (Bruker, 2005); data reduction: SAINT (Bruker, 2005); structure solution: XPREP (Bruker, 2005) and SHELXTL (Bruker, 2000); structure refinement: SHELXTL; molecular graphics: SHELXTL; publication materials: SHELXTL. Neutral atom scattering factors were taken from Cromer and Waber[45]. The crystal is triclinic space group *P*-1, based on the systematic absences, *E* statistics and successful refinement of the structure. The structure was solved by direct methods. Full-matrix least-square refinements minimizing the function $\sum w (F_o^2 - F_c^2)^2$ were applied to the compound. All non-hydrogen atoms were refined anisotropically, except those in the disordered CH_2Cl_2 molecule. All of the H atoms were placed in geometrically calculated positions. The crystal structure data was collected and solved by Ruiyao Wang of Queen's University.

Table 7: Crystal data and structural refinement for 4a

Empirical formula	$C_{74}H_{73}BCl_6NP_3Ru$	
Formula weight	1393.82	
Temperature	180(2) K	
Wavelength	0.71073 Å	
Crystal system	Triclinic	
Space group	P-1	
Unit cell dimensions	a = 9.76550(10) Å	α = 97.4810(10)°.
	b = 15.5381(2) Å	β = 101.6530(10)°.
	c = 23.0015(3) Å	γ = 92.3390(10)°.
Volume	3381.05(7) $Å^3$	
Z	2	
Density (calculated)	1.369 Mg/m^3	
Absorption coefficient	0.583 mm^{-1}	
F(000)	1440	
Crystal size	0.21 x 0.18 x 0.14 mm^3	
Theta range for data collection	2.10 to 26.00°.	
Index ranges	-12<=h<=12, -19<=k<=19, -28<=l<=28	
Reflections collected	27079	
Independent reflections	13208 [R(int) = 0.0320]	
Completeness to theta = 26.00°	99.5 %	
Absorption correction	Multi-scan	
Max. and min. transmission	0.9228 and 0.8873	
Refinement method	Full-matrix least-squares on F^2	
Data / restraints / parameters	13208 / 10 / 796	
Goodness-of-fit on F^2	1.024	
Final R indices [I>2sigma(I)]	R1 = 0.0434, wR2 = 0.1063	
R indices (all data)	R1 = 0.0604, wR2 = 0.1183	
Largest diff. peak and hole	0.649 and -0.843 $e.Å^{-3}$	

3.5.2 Synthesis of $[Bu_4N][RuCl_2(\eta^6\text{-}C_6H_6)\{P^iPr_2(p\text{-}Ph_3BC_6H_4)\}]$, 4a′

Complex **4a′** was prepared in a manner analogous to that described for the synthesis of **4a** except using $[Bu_4N][P^iPr_2(p\text{-}Ph_3BC_6H_4)]$. Yield: 81%. Despite numerous attempts, analytically pure **4a′** could not be obtained. ^1H NMR (499.9 MHz, $CDCl_3$,

22°C): 7.49-6.94 (m, 19H, Ph and PC_6H_4B), 5.22-5.19 (m, 6H, C_6H_6), 3.12 (m, 1H, ^iPr of phosphine) 3.05 (m, 1H, ^iPr of phosphine), 2.78 (m, 8H, Bu), 1.37 (m, 12H, ^iPr of phosphine), 1.28 (m, 16H, Bu), 0.99 (t, 12H, Bu). $^{31}P\{^1H\}$ (202.3 MHz, $CDCl_3$, 22°C): 33.7, 31.8, 29.76 (~1:2:1, all s, P^iPr_2).

3.5.2.1 Reaction of Compound 4a′ with [Et$_4$N][Cl]

A sample of compound **4a′** (0.010 g, 0.01 mmol) was dissolved in $CDCl_3$ (0.5 mL) in a 5 mm NMR tube. Initially, both ^{31}P and ^1H NMR spectra were obtained. $^{31}P\{^1H\}$ (202.3 MHz, $CDCl_3$, 22°C): 32.7, 30.7, 28.6 (~2.5:3.5:2, all s, P^iPr_2). In the initial ^1H spectrum, multiple signals were observed within the η^6-C_6H_6 region (δ = 5.21-5.18 ppm), as reported previously. A portion of [Et$_4$N][Cl] (0.0050 g, 0.03 mmol) was added to the NMR tube and both $^{31}P\{^1H\}$ and ^1H spectra were acquired for the sample. $^{31}P\{^1H\}$ (202.3 MHz, $CDCl_3$, 22°C): 32.5 (s, P^iPr_2). Only one signal in the η^6-C_6H_6 region (δ = 5.20 ppm) were observed after the addition of the excess chloride ions.

3.5.3 Synthesis of [PNP][RuCl$_2$(η^6-C$_6$H$_6$){PPh$_2$(*p*-Ph$_3$BC$_6$H$_4$)}], 4b

Complex **4b** was prepared in a manner analogous to that described for the synthesis of **4a** except using [PNP][PPh_2(*p*-$Ph_3BC_6H_4$)]. Yield: 76%. Despite numerous attempts, analytically pure **4b** could not be obtained. ^1H NMR (499.9 MHz, $CDCl_3$, 22°C): 7.81-6.75 (m, 59H, Ph and PC_6H_4B), 5.24-5.18 (m, 6H, C_6H_6), 2.58 (m, 8H, Bu), 1.20 (m, 8H, Bu), 1.09 (m, 8H, Bu), 0.83 (t, 12H, Bu). $^{31}P\{^1H\}$ (202.3 MHz, $CDCl_3$, 22°C): 22.1 (s, PNP^+), 28.1, 27.5, 26.0 (~3:1:0.5, all s, PPh_2).

3.5.4 Synthesis of [Bu$_4$N][RuCl$_2$(η^6-C$_6$H$_6$){PPh$_2$(*p*-Ph$_3$BC$_6$H$_4$)}], 4b′

Complex **4b′** was prepared in a manner analogous to that described for the synthesis of **4a** except using [Bu_4N][PPh_2(*p*-$Ph_3BC_6H_4$)]. Yield: 88%. Despite numerous

attempts, analytically pure **4b'** could not be obtained. ^{1}H NMR (499.9 MHz, $CDCl_3$, 22°C): 7.70-6.87 (m, 29H, Ph and PC_6H_4B), 5.26-5.21 (m, 6H, C_6H_6), 2.46 (m, 8H, Bu), 1.15 (m, 8H, Bu), 1.08 (m, 8H, Bu), 0.80 (t, 12H, Bu). $^{31}P\{^{1}H\}$ (202.3 MHz, $CDCl_3$, 22°C): 27.4, 25.4, 23.6 (~2:2.5:1.5, all s, PPh_2).

3.5.4.1 Reaction of Compound 4b' with [Et$_4$N][Cl]

A sample of compound **4a'** (0.012 g, 0.01 mmol) was dissolved in $CDCl_3$ (0.5 mL) in a 5 mm NMR tube. Initially, both ^{31}P and ^{1}H NMR spectra were obtained. $^{31}P\{^{1}H\}$ (202.3 MHz, $CDCl_3$, 22°C): 27.4, 25.4, 23.6 (~2:2.5:1.5, all s, PPh_2). In the initial ^{1}H spectrum, there are multiple signals within the η^6-C_6H_6 region (δ = 5.26-5.21 ppm). A portion of [Et$_4$N][Cl] (0.0051 g, 0.03 mmol) was added to the NMR tube and both $^{31}P\{^{1}H\}$ and ^{1}H NMR spectra were acquired for the sample. There was no considerable change observed in the spectra after the addition of the chloride ions compared to the initial sample.

3.5.5 Synthesis of [PNP][RuCl$_2$(η^6-C$_6$H$_6$){PCy$_2$(*p*-Ph$_3$BC$_6$H$_4$)}], 4c

Complex **4c** was prepared in a manner analogous to that described for the synthesis of **4a** except using [PNP][PCy_2(*p*-$Ph_3BC_6H_4$)]. Yield: 91%. Despite numerous attempts, analytically pure **4c** could not be obtained. ^{1}H NMR (499.9 MHz, $CDCl_3$, 22°C): 7.40-6.87 (m, 49H, Ph and PC_6H_4B), 5.28-5.15 (m, 6H, C_6H_6), 2.37-1.16 (m, 22H, Cy of phosphine). $^{31}P\{^{1}H\}$ (202.3 MHz, $CDCl_3$, 22°C): 22.1 (s, PNP^+), 27.5, 26.2, 25.5 (~6:1:0.75, all s, PCy_2).

3.5.6 Synthesis of [Bu$_4$N][RuCl$_2$(η^6-C$_6$H$_6$){PCy$_2$(*p*-Ph$_3$BC$_6$H$_4$)}], 4c'

Complex **4c'** was prepared in a manner analogous to that described for the synthesis of **4a** except using [Bu_4N][PCy_2(*p*-$Ph_3BC_6H_4$)]. Yield: 83%. Despite numerous

attempts, analytically pure **4c'** could not be obtained. ^{1}H NMR (499.9 MHz, $CDCl_3$, 22°C): 7.40-6.87 (m, 19H, Ph and PC_6H_4B), 5.10-5.06 (m, 6H, C_6H_6), 2.61 (m, 8H, Bu), 2.35-1.44 (m, 38H, Bu and Cy of phosphine), 0.90 (t, 12H, Bu). $^{31}P\{^{1}H\}$ (202.3 MHz, $CDCl_3$, 22°C): 26.8, 24.9, 23.2 (~1:2:1, all s, PCy_2).

3.6 Synthesis of $[RuCl(\eta^6\text{-}C_6H_6)\{P^iPr_2(p\text{-}Ph_3BC_6H_4)\}]_2$, 5

In a Schlenk tube, complex **4a** (0.400 g, 0.327 mmol) and AgOTf (0.095 g, 0.370 mmol) was dissolved in THF (15 mL). The brown solution mixture was allowed to stir for 2 hours. During this time a white precipitate of AgCl deposited. Volatiles were removed under reduced pressure and the brown product was redissolved in CH_2Cl_2 (10 mL). The solution was filtered through a short plug of Celite (~2 cm × 1 cm). Volatiles were once again removed to yield a brown product. The product was redissolved in THF (5 mL) followed by a portion of hexanes (1 mL). The solution was vigorously stirred for several minutes to yield a deep dark brown solution with a white precipitate. The mixture was filtered through a short plug of Celite (~2 cm × 1 cm) and volatiles were once again removed under reduced pressure. This purification step was repeated once more to remove the remaining impurities. Yield = 20%. Despite numerous attempts, analytically pure **5** could not be obtained. ^{1}H NMR (499.9 MHz, $CDCl_3$, 22°C): 7.96-7.26 (m, 49H, Ph and PC_6H_4B), 5.35 (s, 6H, C_6H_6), 3.16 (m, 2H, ^{i}Pr of phosphine), 1.49 (m, 6H, ^{i}Pr of phosphine), 1.27 (m, 6H, ^{i}Pr of phosphine). $^{31}P\{^{1}H\}$ (202.3 MHz, $CDCl_3$, 22°C): 33.2 (s, P^iPr_2). [PNP][OTf] from THF/hexanes step: ^{1}H NMR (499.9 MHz, $CDCl_3$, 22°C): 7.36-7.22 (m, 30H, Ph). $^{31}P\{^{1}H\}$ (202.3 MHz, $CDCl_3$, 22°C): 22.3 (s, PNP^+). $^{19}F\{^{1}H\}$ (470.2 MHz, $CDCl_3$, 22°C) : -75.00 (s, OTf).

3.6.1 Reaction of Compound 5 with MeCN

A sample of **5** (0.012 g, 0.01 mmol) was dissolved in 5 mL of MeCN. The solution was allowed to stir for 1 hour, and was followed by the removal of volatiles under reduced pressure. The $^{31}P\{^{1}H\}$ and ^{1}H NMR spectra revealed there was no change from the spectral data observed for compound **5**. A similar reaction was conducted except the the solution was refluxed at 80°C for 2 hours. Once again, there was no spectral change from those observed for compound **5**.

3.6.2 Variable Temperature NMR Experiment with Compound 5

A sample of compound **5** (0.014 g, 0.01 mmol) was dissolved in $C_2D_4Cl_2$ (0.5 mL) in a 5 mm NMR tube fitted with a rubber septum attached to an N_2 line. An initial $^{31}P\{^{1}H\}$ spectrum was acquired at 22°C and the temperature was gradually increased to obtain spectra at 40°C and 60°C. No significant changes were observed up to 60°C.

3.7 Attempted Synthesis of [RuCl(=C=C=CPh$_2$)(η^6-C$_6$H$_6$){P^{i}Pr$_2$(*p*-Ph$_3$BC$_6$H$_4$)}]

Complex **4a** (0.107 g, 0.087 mmol) and 1,1-diphenylpropynol (0.048 g, 0.40 mmol) were dissolved in CH_2Cl_2 (10 mL). Next, MeOTf (11 μL, 0.097 mmol) was added via syringe, producing a red-brown mixture almost immediately. The solution was allowed to stir for 2 hours and during this time the mixture gradually turned a deep, dark red colour. Volatiles were removed under reduced pressure to yield a reddish-brown product. The product was washed with benzene (10 mL) and the red supernatant was cannulated into a clean, degassed flask, leaving behind an oily brown product. Volatiles were once again removed and both flasks were dried under reduced pressure. NMR results for the dark red product indicate three distinct signals in the $^{31}P\{^{1}H\}$ spectrum with the signal at $\delta = 22.3$ ppm being associated to $(PNP)^+$. [$^{31}P\{^{1}H\}$ (202.3 MHz, C_6D_6,

22°C): 32.8, 32.4, 22.3 (~1:1:6, all s)]. ^{1}H NMR (499.9 MHz, C_6D_6, 22°C) revealed two signals in the arene region at $\delta = 4.52$ ppm and $\delta = 4.48$ ppm, indicating two species containing the η^6-C_6H_6 ligand. ^{1}H and $^{31}P\{^{1}H\}$ NMR results for the oily brown product revealed spectra similar to that of compound **5** and [PNP][OTf] [$^{31}P\{^{1}H\}$ (202.3 MHz, C_6D_6, 22°C): 33.1, 22.3 (~1:2.5, both s)]. Attempts to isolate the red product were unsuccessful because of poor yields, and attempts to improve the yield of the reaction were unsuccessful despite numerous variations to the experimental conditions. Variations to the experimental procedure included varying halide abstracting agents to include $AgBF_4$, $AgPF_6$, $AgNO_3$, $NaPF_6$ and NH_4PF_6. Variations to the reagent ratios included 1, 1.5, 2, 2.5, 5, 10 and 100 fold excesses of 1,1-diphenylpropynol to metal and 1, 1.1, 1.2 and 1.5 fold excesses of halide abstracting agent to metal. Three other solvents were used in similar reactions and include methanol, THF and 1,2-dichloroethane. Finally, the temperature of the reaction was elevated to include reactions at 40°C and 80°C, respectively. Each variation to the reaction conditions resulted in a greater number of unidentified species within the $^{31}P\{^{1}H\}$ spectrum. Similar results for the phenyl and cyclohexyl phosphine analogues were observed.

3.8 Attempted Synthesis of [RuCl(=C=CHPh)(η^6-C_6H_6){P^iPr_2(*p*-$Ph_3BC_6H_4$)}]

In a Schlenk tube, complex **4a** (0.110 g, 0.090 mmol) was dissolved in CH_2Cl_2 (10 mL). Next, MeOTf (11 μL, 0.097 mmol) was added via syringe, followed by phenylacetylene (13 μL, 0.12 mmol). The reaction mixture was allowed to stir for 18 hours, and during this time a slight colour change to yellow was noticed. Volatiles were removed under reduced pressure to yield brown solid. Following NMR analysis, two signals were observed in the $^{31}P\{^{1}H\}$ spectrum, with one being associated to $(PNP)^+$(δ =

22.3 ppm). [$^{31}P\{^1H\}$ (202.3 MHz, $CDCl_3$, 22°C): 33.1, 22.3 (~1:7.5, both s)]. Variations to the experimental procedure included varying halide abstracting agents to include MeOTf, $AgBF_4$, $AgPF_6$, $AgNO_3$, $NaPF_6$ and NH_4PF_6. A variety of reagent ratios were used in the experiment to include 1, 1.5, 2, 5 and 10 fold excesses of phenylacetylene to metal and 1, 1.1, 1.2 and 1.5 fold excesses of halide abstracting agent to metal. Three other solvents were used in similar reactions (methanol, THF and 1,2-dichloroethane). Finally, the temperature of the reaction was elevated to include trials at 40°C and 80°C, respectively. Each variation to the reaction conditions resulted in a greater number of unidentified species within the $^{31}P\{^1H\}$ spectrum. Similar results for the phenyl and cyclohexyl phosphine analogues were observed.

3.9.1 Attemped Synthesis of [Ru(MeCN)$_2$(η^6-C_6H_6){P^{i}Pr$_2$(*p*-Ph$_3$BC_6H_4)}][OTf]

Complex **4a** (0.200 g, 0.163 mmol) and AgOTf (0.130 g, 0.506 mmol) were dissolved in MeCN (10 mL). The mixture immediately turned yellow and a white precipitate of AgCl deposited. The solution was allowed to stir for 40 minutes. Volatiles were removed under reduced pressure and redissolved in CH_2Cl_2 (10 mL). The solution was filtered through a short plug of Celite (~2 cm × 1 cm), followed by the removal of the volatiles under reduced pressure to yield a bright yellow solid. The product was redissolved in THF (5 mL) followed by a portion of hexanes (1 mL). The solution was vigorously stirred for several minutes and then cooled in an ice bath for approximately 2 hours. During this time, a white precipitate formed from the yellow solution and the mixture was filtered through a short plug of Celite (~2 cm × 1 cm). Volatiles were once again removed under reduced pressure to yield a yellow powder. NMR analysis of the yellow product showed three signals in the $^{31}P\{^1H\}$ spectrum, with one being associated

to residual [PNP][OTf] [$^{31}P\{^{1}H\}$ (202.3 MHz, $CDCl_3$, 22°C): 39.6, 36.0, 22.2 (~4:4.5:1, all s)]. A variety of halide abstracting agents were also examined including $AgBF_4$, $AgPF_6$ and MeOTf. Variations to the reagent ratios included 2.1, 2.5 and 5 fold excesses of halide abstracting agent to metal and several reactions were performed at 80°C. All variations to the experimental procedure produced a greater number of unidentified species within the $^{31}P\{^{1}H\}$ spectrum. Similar results for the phenyl and cyclohexyl phosphine analogues were observed.

3.9.2 Attempted Synthesis of $[Ru(MeCN)_2(\eta^6\text{-}C_6H_6)\{PPh_2(p\text{-}Ph_3BC_6H_4)\}][BF_4]$

A Schlenk tube was charged with $[Ru(MeCN)_3(\eta^6\text{-}C_6H_6)][BF_4]_2$ (0.100 g, 0.210 mmol) and $[Li][PPh_2(p\text{-}Ph_3BC_6H_4)]\cdot 2THF$ (0.195 g, 0.337 mmol). Next, CH_2Cl_2 (10 mL) was added via syringe and the yellow solution was allowed to stir for 3 hours. During this time, a white precipitate deposited. The solution was then filtered through a short plug of Celite (~2 cm × 1 cm), followed by the removal of the volatiles under reduced pressure to yield a bright yellow solid. The product was redissolved in CH_2Cl_2 (3 mL) and the product was precipitated out of solution by the addition of hexanes (10 mL) and dried *in vacuo*. One phosphorus-containing species was observed in the $^{31}P\{^{1}H\}$ spectrum [$^{31}P\{^{1}H\}$ (202.3 MHz, $CDCl_3$, 22°C): 33.7 (s, PPh_2)]. Within the ^{1}H NMR spectrum, there was only one signal found in the $\eta^6\text{-}C_6H_6$ region at δ = 5.48 ppm and only one MeCN signal found at δ = 1.49 ppm. A large singlet at δ = 5.35 ppm indicates that the product is solvated with a significant amount of CH_2Cl_2. Several different methods of purification were employed including solvent washes, precipitation reactions, ion exchanges, and recrystallizations which proved unsuccessful in isolating a pure product.

3.9.3 Attempted Synthesis of $[Ru(MeCN)_2(\eta^6\text{-}C_6H_6)\{P^iPr_2(p\text{-}Ph_3BC_6H_4)\}][BF_4]$

In a Schlenk tube, $[Ru(MeCN)_3(\eta^6\text{-}C_6H_6)][BF_4]_2$ (0.010 g, 0.021 mmol) and $[PNP][P^iPr_2(p\text{-}Ph_3BC_6H_4)]$ (0.025 g, 0.026 mmol) were dissolved in CH_2Cl_2 (5 mL). The yellow solution was allowed to stir for 15 minutes. It was then filtered through a short plug of Celite (~2 cm × 1 cm). Volatiles were removed under reduced pressure to yield a bright yellow product. Three distinct signals were observed in the $^{31}P\{^1H\}$ spectrum with the signal at δ = 22.2 ppm being associated to $(PNP)^+$. [$^{31}P\{^1H\}$ (202.3 MHz, $CDCl_3$, 22°C): 35.7, 33.3, 22.2 (~4:1:16.5, all s)]. In the ^1H NMR spectrum, there were two signals in the $\eta^6\text{-}C_6H_6$ region at δ = 5.73 ppm and δ = 5.67 ppm (~1:1, both s). There were a number of MeCN signals found in the ^1H spectrum ranging from δ = 1.41 ppm to 1.27 ppm. Allowing the reaction to proceed for a longer period of time resulted in the formation of several different phosphorus signals within the $^{31}P\{^1H\}$ NMR spectrum. Several different methods of purification were employed including solvent washes, precipitation reactions, ion exchanges, and recrystallizations which proved unsuccessful in isolating one pure product.

4. Results and Discussion

In order to understand the properties and explore applications of the (phosphino)tetraphenylborate ligands, the fundamental coordination chemistry of these ligands as a part of ruthenium-arene complexes was explored during the initial stages of this project.

4.1 Synthesis and Chemistry of [E][$RuCl_2(\eta^6$-*p*-cymene){PR_2(*p*-$Ph_3BC_6H_4$)}] (R = Cy, E = PNP^+, **1a**; R = Cy, E = Bu_4N^+, **1a'**)

The Spivak lab had previously prepared a new cyclohexyl variant of the phosphine [PR_2(*p*-$Ph_3BC_6H_4$)]$^-$. In an attempt to expand upon our work involving reactions between [PR_2(*p*-$Ph_3BC_6H_4$)]$^-$ and [$RuCl_2(\eta^6$-*p*-cymene)]$_2$[43], and possibly gain further insight into the products obtained from these reactions, it was decided that this reaction would be extended to include [PCy_2(*p*-$Ph_3BC_6H_4$)]$^-$. Thus, addition of two equivalents of [PCy_2(*p*-$Ph_3BC_6H_4$)]$^-$ to a CH_2Cl_2 solution containing [$RuCl_2(\eta^6$-*p*-cymene)]$_2$ resulted in the chloride bridge being cleaved, and yielded spectroscopically pure, air-stable, orange-red powders of the monomeric half-sandwich complexes **1a** and **1a'** in good yields (e.g. 77%-92%) (Scheme 13).

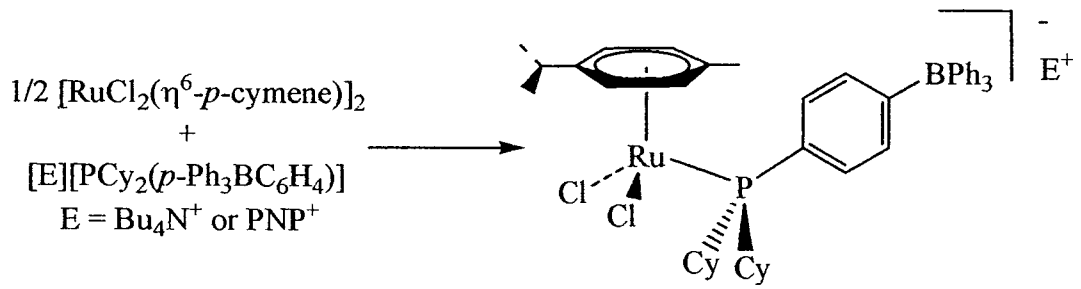

Scheme 13: Synthetic strategy to forming compounds 1a and 1a'

NMR spectroscopic analysis of compounds **1a** and **1a′** unexpectedly revealed complicated spectra. The ^{1}H NMR spectra for both **1a** and **1a′** showed multiple sets of closely spaced signals pertaining to the *ortho* and *meta* arene hydrogen atoms of the η^6-*p*-cymene ligand, rather than the single pair of doublets typically observed for neutral $[RuCl_2(\eta^6\text{-}p\text{-cymene})(PR_3)]$ compounds[29]. The multiple sets of arene signals for compounds **1a** and **1a′** ranged from δ = 5.05 to 4.81 ppm and δ = 5.09 to 4.84 ppm, respectively. The methyl and isopropyl groups of the arene ligand for compound **1a** were found at δ = 2.75 ppm (septet, methine hydrogen of the isopropyl group), 1.84 ppm (singlet, methyl hydrogens of *p*-cymene), 1.79 ppm (singlet, methyl hydrogens of *p*-cymene), 1.77 ppm (singlet, methyl hydrogens of *p*-cymene) and 1.06 ppm (doublet, methyl hydrogens of *p*-cymene). The ^{1}H NMR spectrum for compound **1a′** contained similar signals and chemical shifts for the methyl and isopropyl groups of the arene ligand, and also contained butyl signals of the Bu_4N^+ counterion at δ = 2.69 ppm, 0.99 ppm and two other signals among the crowded cyclohexyl signals between δ = 2.14 ppm and 1.24 ppm (Figure 6). The phenyl region of the ^{1}H NMR spectra for **1a** and **1a′** were observed at δ = 7.61 to 6.85 ppm and δ = 7.43 to 6.93 ppm, respectively. However, the $^{31}P\{^1H\}$ NMR spectra were much more revealing, with each complex producing three closely spaced singlets with varying peak intensities (Figure 5). A typical $^{31}P\{^1H\}$ NMR spectrum for a $[RuCl_2(\eta^6\text{-}p\text{-cymene})(PR_3)]$ complex bearing more traditional neutral phosphines would contain a lone singlet[46]. The signals within the $^{31}P\{^1H\}$ NMR spectra for compounds **1a** and **1a′** were found at δ = 21.9, 20.5, 19.1 ppm (~6:4:1) and δ = 21.4, 19.9, 18.6 ppm (~1.5:2.5:1), respectively. For compound **1a**, there was an additional singlet in the $^{31}P\{^1H\}$ NMR spectrum at δ = 22.1 ppm pertaining to the PNP^+ counterion.

Interestingly, the relative peak intensities of the three signals change depending on the counterion present. When the larger PNP^+ counterion is present the peak intensity ratio of ~6:4:1 is observed, while the presence of the Bu_4N^+ counterion results in a more evenly distributed ratio of ~1.5:2.5:1.

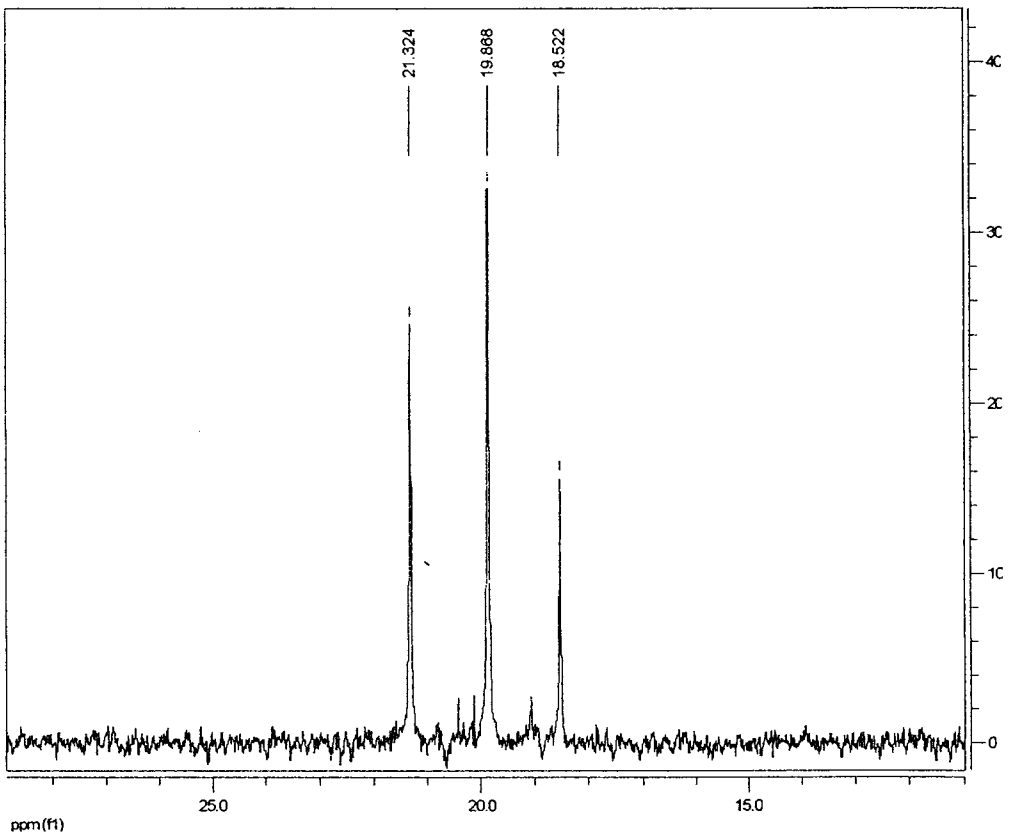

Figure 5: $^{31}P\{^1H\}$ NMR spectrum of compound 1a′

Spectral evidence indicates there exists multiple ruthenium species in solution; notwithstanding the combustion analysis indicates only [E][$RuCl_2(\eta^6$-*p*-cymene){PCy_2(*p*-$Ph_3BC_6H_4$)}] (E = PNP^+, **1a**; Bu_4N^+, **1a′**) in the solid state. At this point in the project, there were two proposed scenarios for the multiple signals observed in the NMR spectra. The first proposed explanation involved the presence of rotational isomers formed in solution.

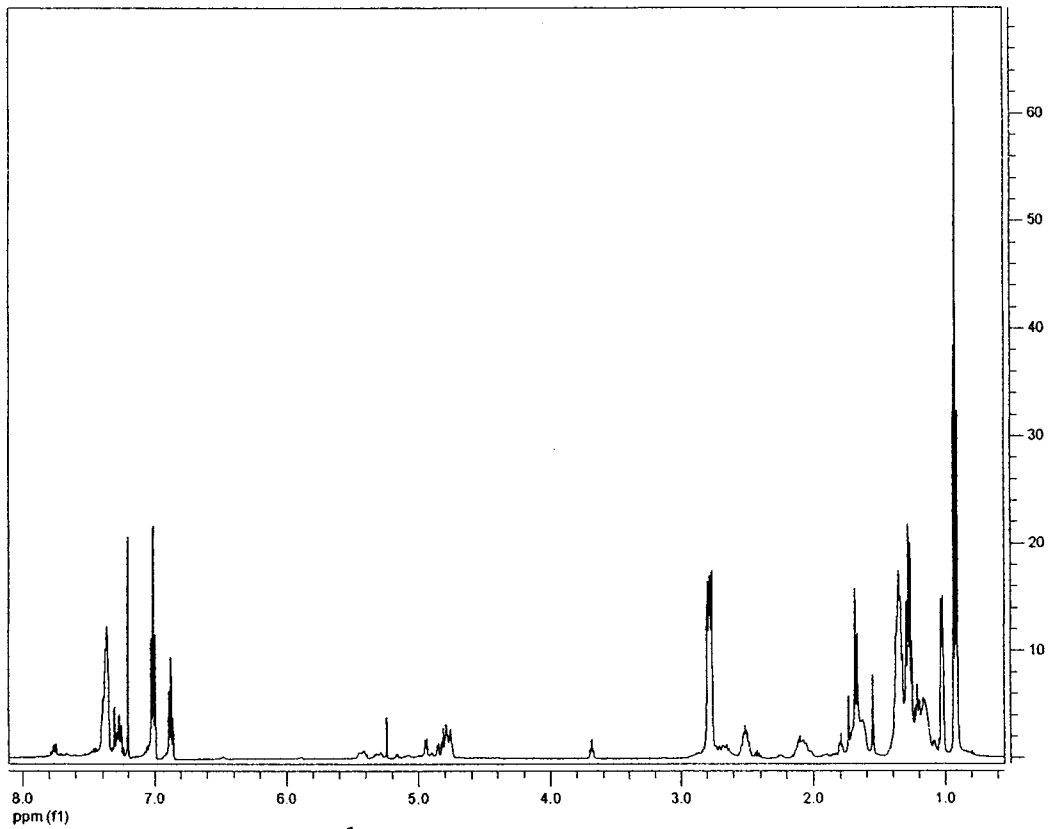

Figure 6: ^{1}H NMR spectrum of compound 1a′

Rotational isomers would be a result of restricted rotation about the ruthenium-phosphorus bond, most likely a consequence of the relatively bulky substituents of the anionic tertiary phosphine. Although there are no documented cases of hindered rotation about metal-phosphorus bonds in ruthenium-arene complexes, there are a few examples of other metal-arene complexes exhibiting rotational isomers[47]. A series of variable temperature NMR studies were performed in an attempt to gain insight into the unique spectroscopic observations for compounds **1a** and **1a′**. An NMR sample was prepared by dissolving compound **1a′** in $C_2D_4Cl_2$ under an atmosphere of N_2 gas. An initial $^{31}P\{^{1}H\}$ spectrum was acquired at 20 °C, followed by a gradual increase in temperature to obtain spectra at 40 °C, 60 °C and 80 °C. There were no obvious changes among the $^{31}P\{^{1}H\}$ NMR spectra acquired between 20 °C and 80 °C. Signals associated with rotational

isomers would be expected to coalescence as the energetic threshold restricting the rotation about the metal-phosphorus bond is exceeded at higher temperatures[47]. Since elevating the temperature of the NMR sample containing compound **1a'** resulted in no visible change in the $^{31}P\{^{1}H\}$ spectrum, the presence of rotational isomers was ruled out.

The second possible explanation for the unique observations is the formation of monomer-dimer equilibria (Scheme 14). Formation of monomer-dimer equilibria could be achieved through spontaneous chloride ligand dissociation from the monomeric species (**A**) to yield a dimeric species bridged through one chloride ligand (**B**), followed by the dissociation of another chloride ligand to yield a dimer bridged through two chloride ligands (**C**). There is evidence of ruthenium-arene complexes forming *in situ* monomer-dimer equilibria facilitated by spontaneous chloride ligand dissociation[40]. Furthermore, mono- and dichloride bridged ruthenium-arene complexes are not without precedent[29, 35-38, 41], and this makes this proposed scenario more plausible.

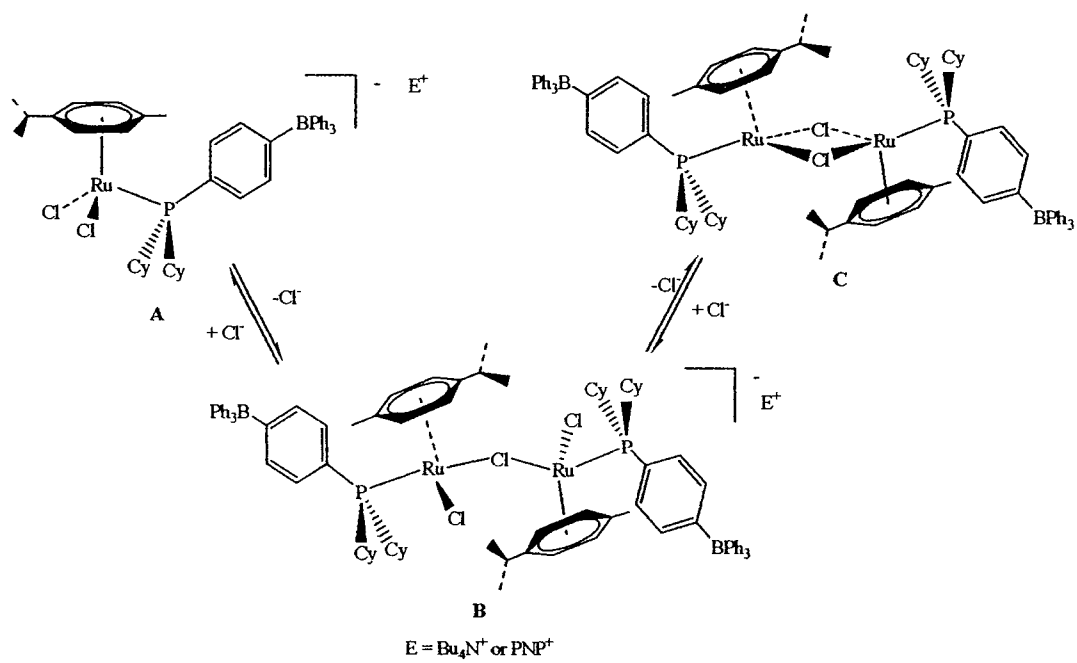

Scheme 14: Proposed monomer-dimer equilibria for compounds 1a and 1a'

An alternate explanation for the observations is the formation complexes **A** and **B**, with two diastereomers of **B** being present in solution. Several attempts to produce a single crystal of compounds **1a** and **1a′** for X-ray diffraction were unsuccessful; all attempts yielded brown oily products.

4.2 Synthesis of [RuCl(py)(η^6-*p*-cymene){PCy_2(*p*-$Ph_3BC_6H_4$)}], 2 and [RuCl(MeCN)(η^6-*p*-cymene){PCy_2(*p*-$Ph_3BC_6H_4$)}], 3

Attention was turned towards trapping the 16-electron complex [RuCl(η^6-*p*-cymene){PCy_2(*p*-$Ph_3BC_6H_4$)}] with MeCN or py, and exploring the synthesis of zwitterionic complexes using these ligands. For example, the synthesis of neutral complexes was achieved by selectively removing a chloride ligand from compound **1a** in the presence of a trapping ligand (Scheme 15). Two different neutral, zwitterionic 18-electron complexes were formed through this synthetic approach. Complexes **2** and **3** were characterized via ^1H and $^{31}P\{^1H\}$ NMR spectroscopy and combustion analyses. It is important to note that an extremely large excess of trapping ligand was required for the formation of both complexes, for example, 100-fold excess. In both cases, similar reactions containing only two or three fold excess of trapping ligand yielded two $^{31}P\{^1H\}$ signals. One signal can be attributed to a small amount of the desired product, and the other signal had a chemical shift of $\delta = 21.4$ ppm, which has a similar shift to those of the starting material (**1a**). Looking at the $^{31}P\{^1H\}$ NMR spectra for compounds **2** and **3**, there is only one phosphorus signal in the $^{31}P\{^1H\}$ spectra for both compounds at $\delta = 27.51$ ppm (Figure 7) and $\delta = 29.72$ ppm (Figure 9), respectively. These signals appear downfield from precursor **1a**. The presence of one phosphorus signal in the $^{31}P\{^1H\}$

spectra for both compounds is expected for complexes containing a single phosphorus ligand, but is in stark contrast to what was observed for **1a** and **1a'**.

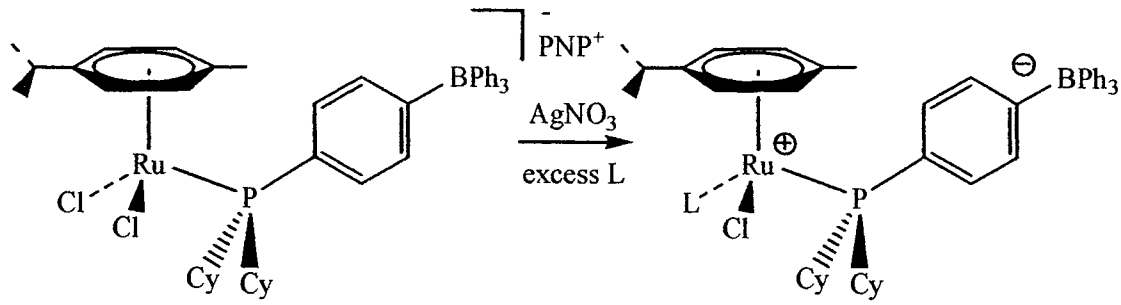

L = py (**2**) or MeCN (**3**)

Scheme 15: Synthetic approach to forming compounds 2 and 3

In the ^{1}H NMR spectra for compounds **2** and **3,** the chirality of the metal centres was established by the diastereotopic methyl signals of the isopropyl substituent, and the inequivalent arene hydrogen atoms of the η^6-*p*-cymene ligand[28b]. The ^{1}H NMR spectra for compounds **2** (Figure 8) and **3** (Figure 10) contained four individual signals pertaining to the *ortho* and *meta* arene hydrogen atoms of the η^6-*p*-cymene ligand which ranged from δ = 5.41 ppm to 4.82 ppm (each dublet) and δ = 5.33 ppm to 4.96 ppm (each dublet), respectively. The signals associated with the pyridine ligand of compound **2** were observed at δ = 8.86 ppm (broad) and within the crowded phenyl region ranging from δ = 7.88 ppm to 6.97 ppm. The ortho-pyridine hydrogens at δ = 8.86 ppm are diagnostic of coordinated pyridine[48]. Lastly, the signal pertaining to the MeCN ligand of compound **3** was observed at δ = 1.54 ppm (singlet) and is typical for coordinated MeCN[49]. Numerous attempts to grow single crystals for X-ray diffraction were unsuccessful despite varying solvent combinations and temperature conditions.

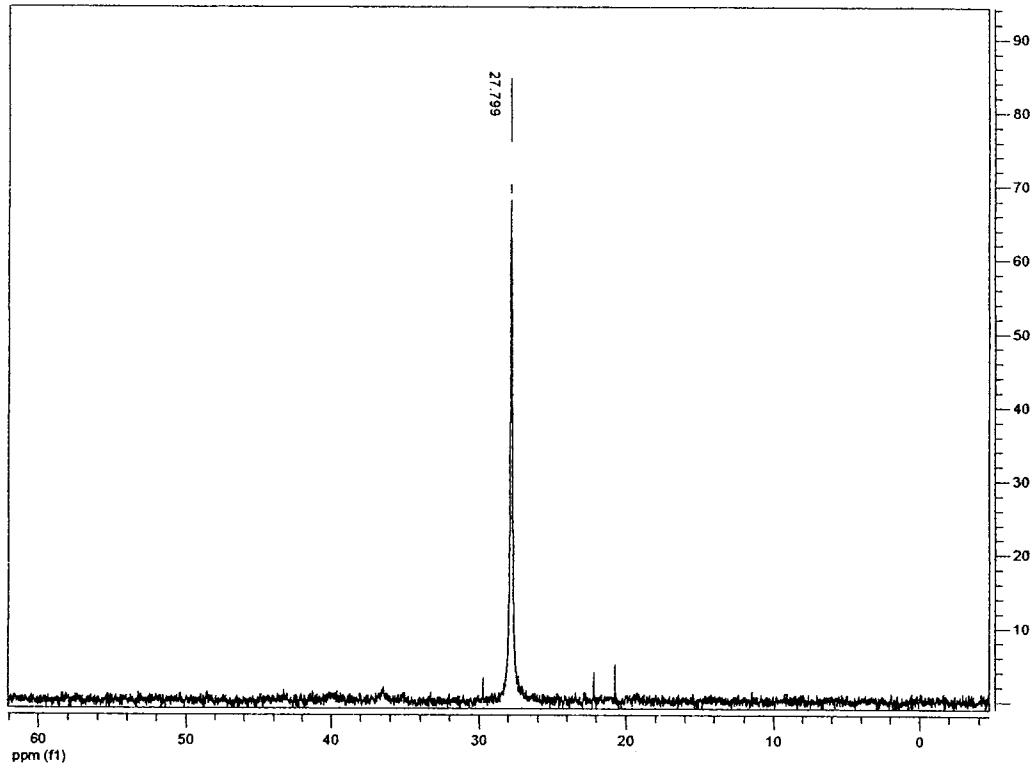

Figure 7: $^{31}P\{^{1}H\}$ NMR spectrum of compound 2

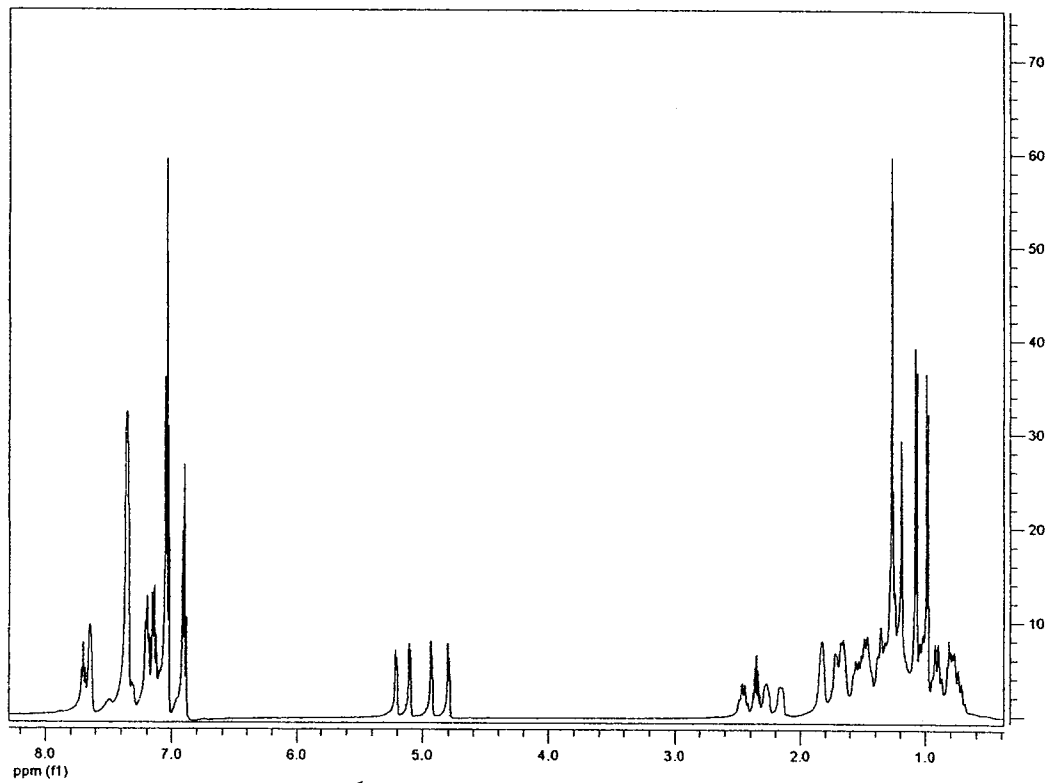

Figure 8: ^{1}H NMR spectrum of compound 2

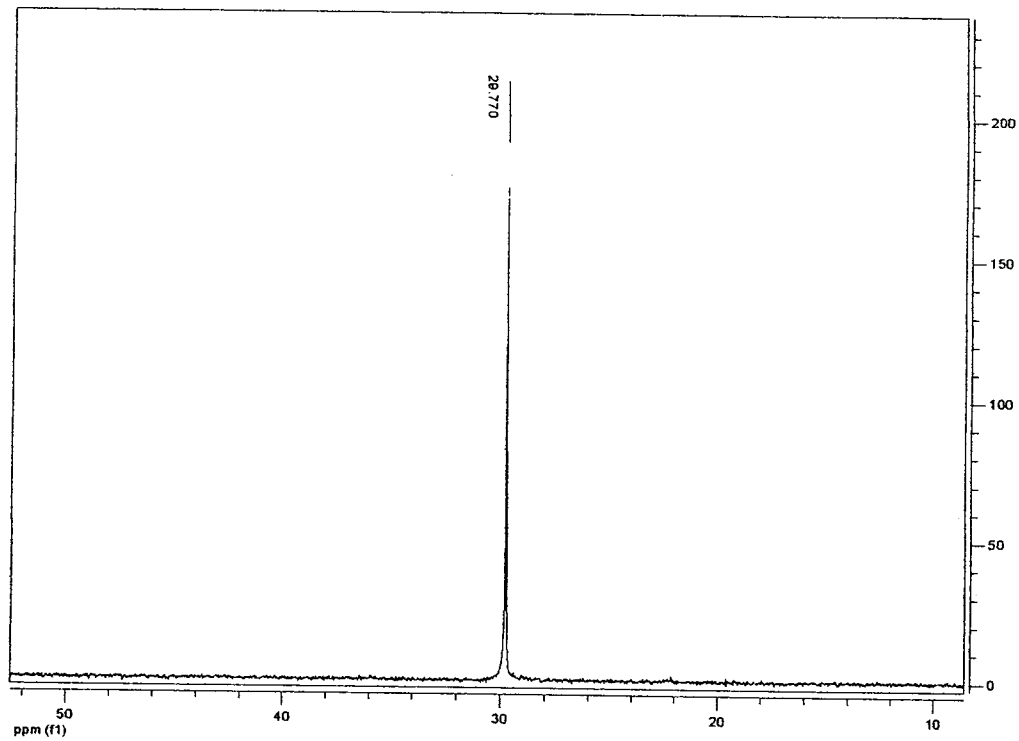

Figure 9: $^{31}P\{^{1}H\}$ NMR spectrum of compound 3

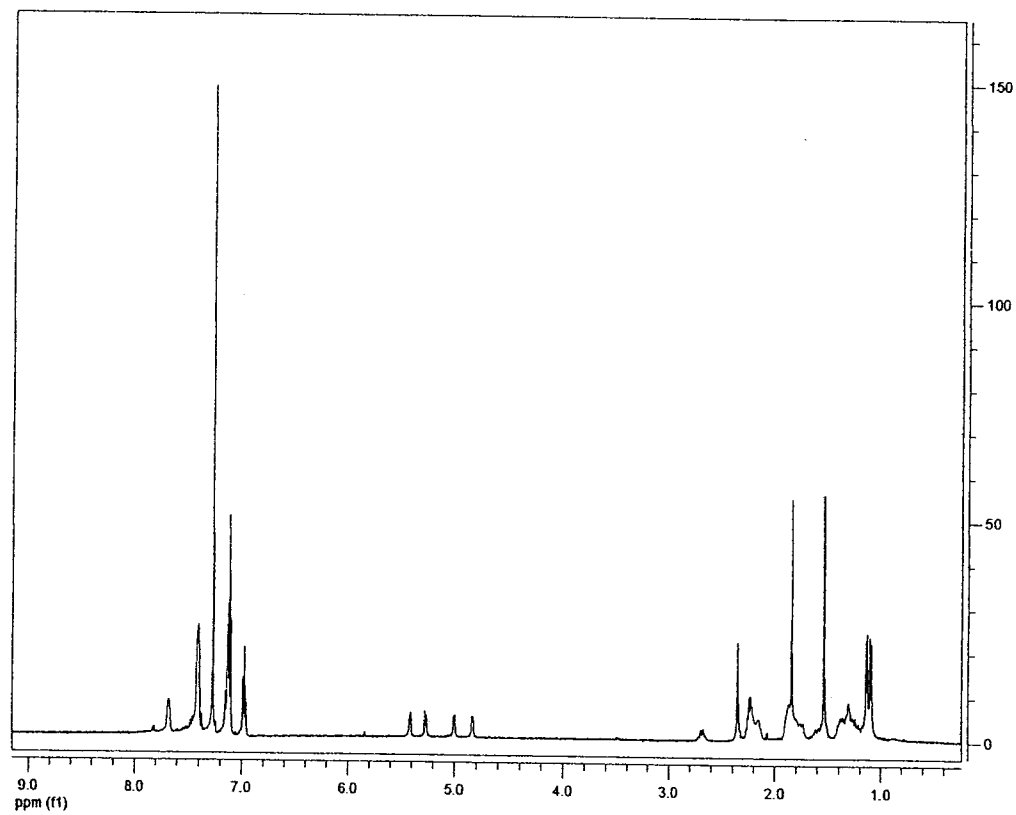

Figure 10: ^{1}H NMR spectrum of compound 3

4.3 Synthesis and Chemistry of [E][$RuCl_2(\eta^6\text{-}C_6H_6)\{PR_2(p\text{-}Ph_3BC_6H_4)\}$] (R = ^{i}Pr, E = PNP^+, **4a**; R = ^{i}Pr, E = Bu_4N^+, **4a′**; R = Ph, E = PNP^+, **4b**; R = Ph, E = Bu_4N^+, **4b′**; R = Cy, E = PNP^+, **4c**; R = Cy, E = Bu_4N^+, **4c′**)

In the second phase of the project, attention was directed towards expanding synthetic investigations to include a different type of arene ligand. Due to the availability of $[RuCl_2(\eta^6\text{-}C_6H_6)]_2$, the $\eta^6\text{-}C_6H_6$ ligand was the second type of arene ligand to be incorporated as a co-ligand with the anionic phosphine. The $\eta^6\text{-}C_6H_6$ ligand also provided a number of advantages including simpler ^{1}H NMR spectra, particularly in the arene region and a less-bulky arene ligand, as the substituents on the η^6-*p*-cymene ligand might be causing restricted rotation. A similar synthetic approach to that of **1a** and **1a′** was employed to produce the desired anionic ruthenium arene complexes (Scheme 16). The addition of two equivalents of $[PR_2(p\text{-}Ph_3BC_6H_4)]^-$ (R = Ph, Cy, or ^{i}Pr) with $[RuCl_2(\eta^6\text{-}C_6H_6)]_2$ yielded spectroscopically pure, air-stable, brown powders in good yields (76%-91%).

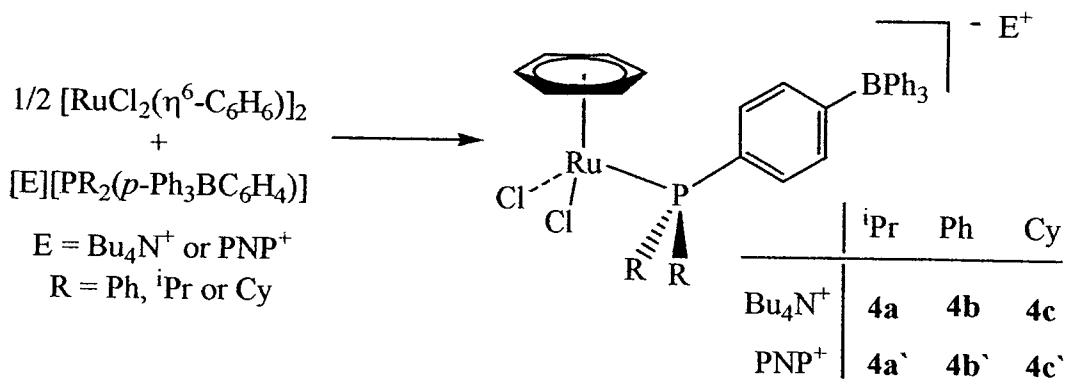

Scheme 16: Synthetic approach to forming compounds 4a-4c′

Complexes **4a-4c** and **4a′-4c′** were characterized in solution via ^{1}H and $^{31}P\{^1H\}$ NMR spectroscopy. Similar to compounds **1a** and **1a′**, intriguing NMR data were observed for compounds **4a-4c** and **4a′-4c′**. Within the ^{1}H NMR spectra, there are

multiple closely spaced signals in the arene region pertaining to the η^6-C_6H_6 ligand. For compounds **4a-4c** and **4a′-4c′**, the arene hydrogen atom signals ranged from δ = 5.28 ppm to 5.06 ppm, with each set of arene signals varying by no more than 0.13 ppm. A typical ^{1}H spectrum for a complex with a η^6-C_6H_6 ligand would exhibit a singlet, as all the hydrogen atoms of the η^6-C_6H_6 ligand would be equivalent[50]. Each ^{1}H NMR spectrum for compounds **4a-4c** and **4a′-4c′** also contains the appropriate signals associated to the groups of the substituted tertiary phosphine. For compounds **4a**, the isopropyl signals of the phosphine are located at δ = 3.12 ppm and δ = 3.05 ppm; for compound **4a′**, the isopropyl signals of the phosphine are located at δ = 3.07 ppm and δ = 2.78 ppm. For compounds **4b** and **4b′**, the phenyl signals of the phosphine are found in the crowded phenyl region of the ^{1}H NMR spectrum and range from δ = 7.81 ppm to 6.75 ppm and δ = 7.70 ppm to 6.87 ppm, respectively. Lastly, the cyclohexyl signals of the phosphine for compounds **4c** and **4c′** ranged from δ = 2.37 ppm to 1.16 ppm and δ = 2.35 ppm to 1.44 ppm, respectively.

In addition to the complex ^{1}H NMR spectra, the ^{31}P{^{1}H} NMR spectra for compounds **4a-4c** and **4a′-4c′** were equally complex. All ^{31}P{^{1}H} NMR spectra for compounds **4a-4c** and **4a′-4c′** contained three closely spaced singlets with varying peak intensities and the relative peak intensities differ depending on the counterion present. The presence of the Bu_4N^+ counterion resulted in more evenly distributed peak intentities. The signals found in the ^{31}P{^{1}H} NMR spectra for compounds **4a-4c** were: δ = 34.3 ppm, 33.8 ppm and 33.3 ppm (~6:1.5:1); δ = 28.1 ppm, 27.5 ppm and 26.0 ppm (~3:1:0.5); and δ = 27.5 ppm, 26.2 ppm and 25.5 ppm (~6:1:0.75), respectively, while the signals for compounds **4a′-4c′** were observed at δ = 33.7 ppm, 31.8 ppm and 29.76 ppm (~1:2:1); δ

= 27.4 ppm, 25.4 ppm and 23.6 ppm (~2:2.5:1.5); and δ = 26.8 ppm, 24.9 ppm and 23.2 ppm (~1:2:1), respectively. A PNP^+ counterion signal at δ = 22.1 ppm was present in the $^{31}P\{^1H\}$ NMR spectra for compounds **4a**, **4b** and **4c**. Thus, spectral evidence suggests there exists multiple ruthenium species in solution. Much like what was observed for **1a** and **1a'**, monomer-dimer equilibria appear to exist also for **4a-4c** and **4a'-4c'** in solution (Scheme 17).

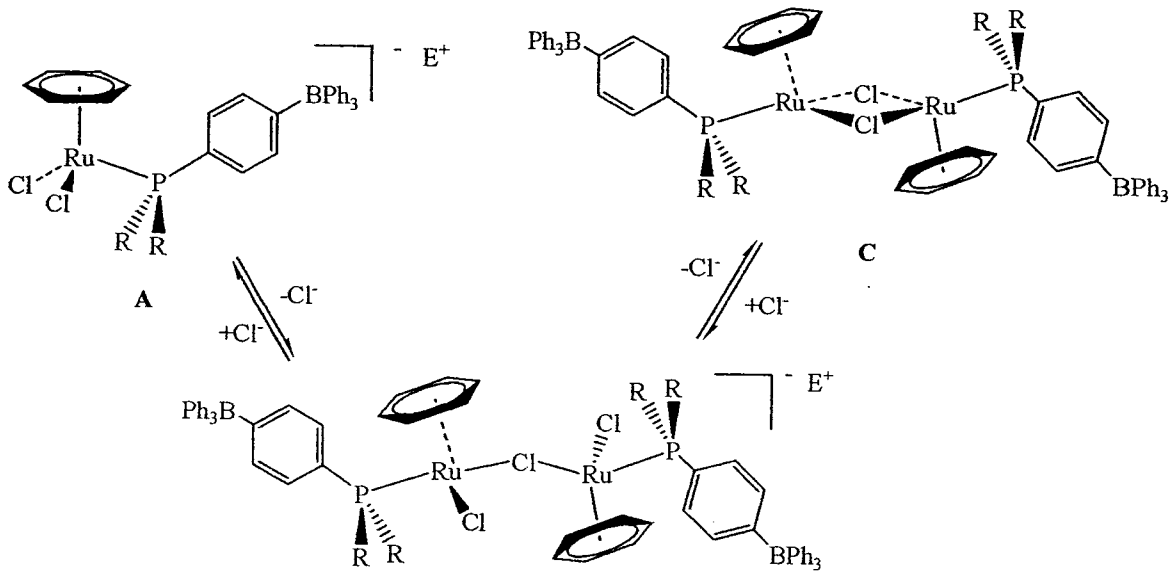

E = Bu_4N^+ or PNP^+
R = Ph, ^{i}Pr or Cy

Scheme 17: Proposed *in situ* monomer-dimer equilibria for compounds 4a-4c'

Numerous attempts under various conditions were employed to produce a quality single crystal for X-ray diffraction. Generally, brown oily products were obtained. Despite this, X-ray-quality single crystals of **4a** were obtained by slow diffusion of hexanes into a concentrated solution of **4a** in CH_2Cl_2. The ruthenate(II) anion of **4a** is displayed in Figure 11. As expected, the ruthenium centre of **4a** exhibits a three-legged piano-stool coordination geometry, which is often observed for $[RuCl_2(\eta^6\text{-arene})(PR_3)]$

complexes[51]. The solid-state structure of **4a** reveals a number of interesting aspects of the anionic ruthenium complex and can be compared to similar compounds (Table 8). A pseudo-octahedral geometry is formed about the metal centre as the η^6-C_6H_6 ligand occupies three facial coordination sites, in concurrence with the approximate 90° angles associated to P(1)-Ru(1)-Cl(1) (89.59(3)°), P(1)-Ru(1)-Cl(2) (88.20(3)°) and Cl(1)-Ru(1)-Cl(2) (88.14(3)°) bond angles. The bond angles are similar to those observed for [Ru(η^6-C_6H_6)Cl_2(PPh_3)], where the bond angles for P(1)-Ru(1)-Cl(1, P(1)-Ru(1)-Cl(2) and Cl(1)-Ru(1)-Cl(2) are 86.15(4)°, 86.15(4)° and 88.18(3)°, respectively[52]. The bond distances between the ruthenium and the carbon atoms of the arene ligand for compound **4a** are asymmetric, with bond distances Ru(1)-C(1), Ru(1)-C(2), Ru(1)-C(3), Ru(1)-C(4), Ru(1)-C(5) and Ru(1)-C(6) being 2.179(4) Å, 2.191(3) Å, 2.164(4) Å, 2.172(4) Å, 2.242(4) Å and 2.255(3) Å, respectively. Similar bond distances are observed for [Ru(η^6-C_6H_6)Cl_2(PPh_3)] with bond distances Ru(1)-C(1), Ru(1)-C(2), Ru(1)-C(3), Ru(1)-C(4), Ru(1)-C(5) and Ru(1)-C(6) being 2.228(3) Å, 2.193(3) Å, 2.201(3) Å, 2.172(3) Å, 2.203(3) Å and 2.214(3) Å, respectively. Differences in the bond distances of compound **4a** can be related to the large *trans* influence being applied by the anionic phosphine ligand[19,53]. One might expect the C-C bond distances of the arene ligand to be longer for complexes containing a stronger donating phosphine since the arene ligand can back-bond, however this is not the case for **4a**. The C(1)-C(2), C(1)-C(6), C(2)-C(3), C(3)-C(4), C(4)-C(5) and C(5)-C(6) bond distances for **4a** were determined to be 1.377(5) Å, 1.418(5) Å, 1.398(6) Å, 1.383(6) Å, 1.424(6) Å and 1.371(6) Å, respectively, whereas the bonds for [Ru(η^6-C_6H_6)Cl_2(PPh_3)] were determined to be 1.408(5) Å, 1.380(4) Å, 1.382(5) Å, 1.400(6) Å, 1.400(4) Å and 1.407(4) Å, respectively. The Ru(1)-P(1), Ru(1)-

Cl(1) and Ru(1)-Cl(2) bond distances were determined to be 2.3896(8) Å, 2.4323(8) Å and 2.4371(8) Å, respectively, and are similar to those observed for neutral [$RuCl_2(\eta^6$-arene)(PR_3)] complexes[35,53, 52]. For example, Ru(1)-P(1), Ru(1)-Cl(1) and Ru(1)-Cl(2) bond distances for [$Ru(\eta^6$-$C_6H_6)Cl_2(PPh_3)$] were determined to be 2.3637(2) Å, 2.406(2) Å and 2.4118(10) Å, respectively. Surprisingly, the substituent containing the bulky BPh_3 group is situated near the arene ligand, which likely resulted from packing effects. One would assume the cumbersome BPh_3 group would be positioned away from the arene ligand to a less occupied region for steric reasons; however this is not the case. Lastly, the complex was solvated with two CH_2Cl_2 molecules within the unit cell.

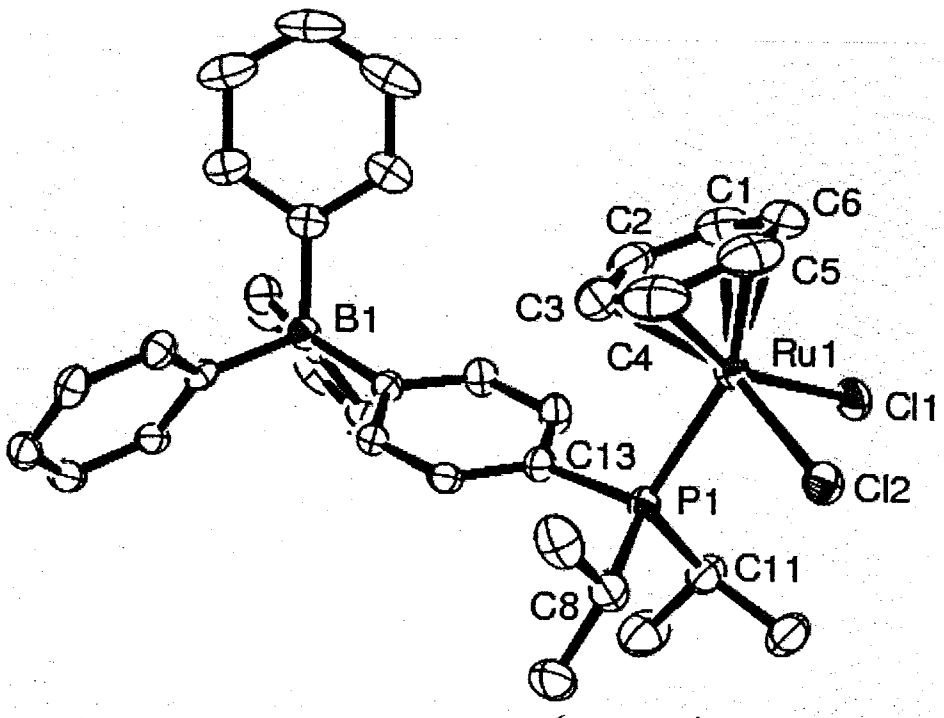

Figure 11: ORTEP drawing of [PNP][$RuCl_2(\eta^6$-C_6H_6){P ^{i}Pr$_2$(p-$Ph_3BC_6H_4$)}], 4a (H atoms, PNP^+ counterion and CH_2Cl_2 solvate omitted for clarity)

Table 8: Selected bond lengths and bond angles for [PNP][$RuCl_2(\eta^6\text{-}C_6H_6)\{P^iPr_2(p\text{-}Ph_3BC_6H_4)\}$], 4a

Selected Bond Lengths (Å)	Selected Bond Angles (°)
Ru(1)-P(1), 2.3896(8)	P(1)-Ru(1)-Cl(1), 89.59(3)
Ru(1)-Cl(1), 2.4323(8)	P(1)-Ru(1)-Cl(2), 88.20(3)
Ru(1)-Cl(2), 2.4371(8)	Cl(1)-Ru(1)-Cl(2), 88.14(3)
Ru(1)-C(1), 2.179(4)	
Ru(1)-C(2), 2.191(3)	
Ru(1)-C(3), 2.164(4)	
Ru(1)-C(4), 2.172(4)	
Ru(1)-C(5), 2.242(4)	
Ru(1)-C(6), 2.255(3)	
C(1)-C(2), 1.377(5)	
C(1)-C(6), 1.418(5)	
C(2)-C(3), 1.398(6)	
C(3)-C(4), 1.383(6)	
C(4)-C(5), 1.424(6)	
C(5)-C(6), 1.371(6)	

Despite several attempts, analytically pure samples of **4a-4c** and **4a′-4c′** could not be obtained. A variety of purification techniques including filtrations, recrystallizations and solvent washes were employed to purify already spectroscopically pure samples of

compounds **4a-4c** and **4a′-4c′**, but all attempts were unsuccessful in acquiring analytically pure samples.

4.4 NMR Experiment: Compound 4a′ with [Et$_4$N][Cl]

A series of NMR experiments were employed in an attempt to shed more light on the equilibria observed for **4a-4c** and **4a′-4c′**. If there are monomer-dimer equilibria in solution, then they should be sensitive to the concentration of Cl^- in solution. Compound **4a′** was chosen for the experiment because a pure sample was readily available at the time of the experiment. An NMR sample containing compound **4a′** was treated with a three-fold excess of [Et$_4$N][Cl]. As noted in previous sections, there are three closely spaced singlets at δ = 32.7 ppm, 30.7 ppm and 28.6 ppm in the $^{31}P\{^1H\}$NMR spectrum with varying intensities, and multiple signals found in the arene region (δ = 5.21 ppm to 5.18 ppm) pertaining to the η^6-C_6H_6 ligand for pure **4a′**. A visible change in the $^{31}P\{^1H\}$ NMR spectrum is observed after the addition of the chloride to the $CDCl_3$ solution. After the addition, one dominant signal is observed in the $^{31}P\{^1H\}$ NMR spectrum at δ = 32.5 ppm (Figure 12). A similar observation is found in the arene region of the ^1H NMR spectrum (Figure 13); one dominant signal in the η^6-arene region (δ = 5.20 ppm) is observed after the addition of the excess chloride ions, which is what is expected for $[RuCl_2(\eta^6\text{-}C_6H_6)(PR_3)]$[54].

A similar NMR experiment was performed for compound **4b′**, however no significant changes were observed in the ^1H and $^{31}P\{^1H\}$ NMR spectra after the addition of excess [Et$_4$N][Cl]. This different response towards added chloride ions might be linked to the electron donating ability of the phosphine ligand. We might expect $[Ph_2PC_6H_4BPh_3]^-$ in **4b′** to be a relatively weaker donor ligand compared to

$[^{i}Pr_2PC_6H_4BPh_3]^-$ in **4a′**, making chloride dissociation less favourable, thus favouring the formation of the monomeric species. The addition of excess chloride ions would thus show minimal effects in the equilibrium. At this time, it is difficult to establish exactly what is happening in solution for these compounds and requires further investigation.

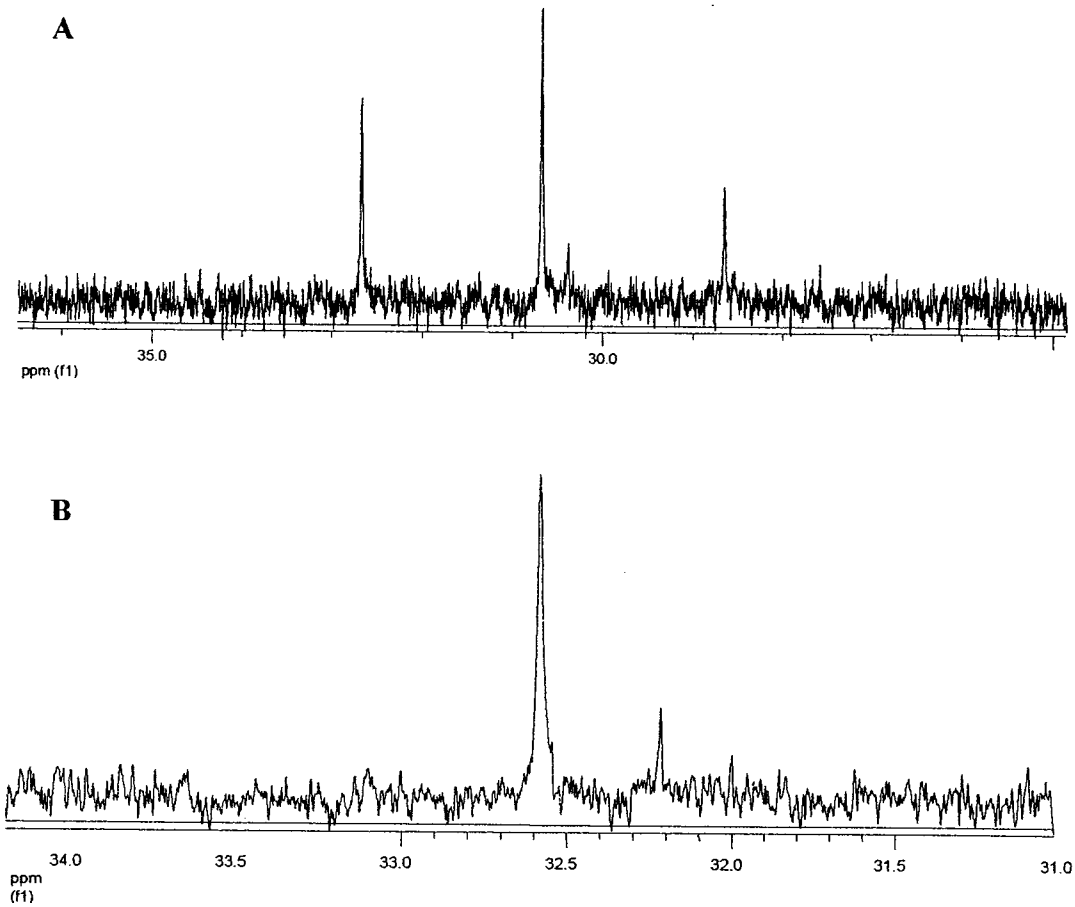

Figure 12: $^{31}P\{^{1}H\}$ NMR spectrum of complex 4a′ (A) and 4a′ in the presence of excess chloride ions (B)

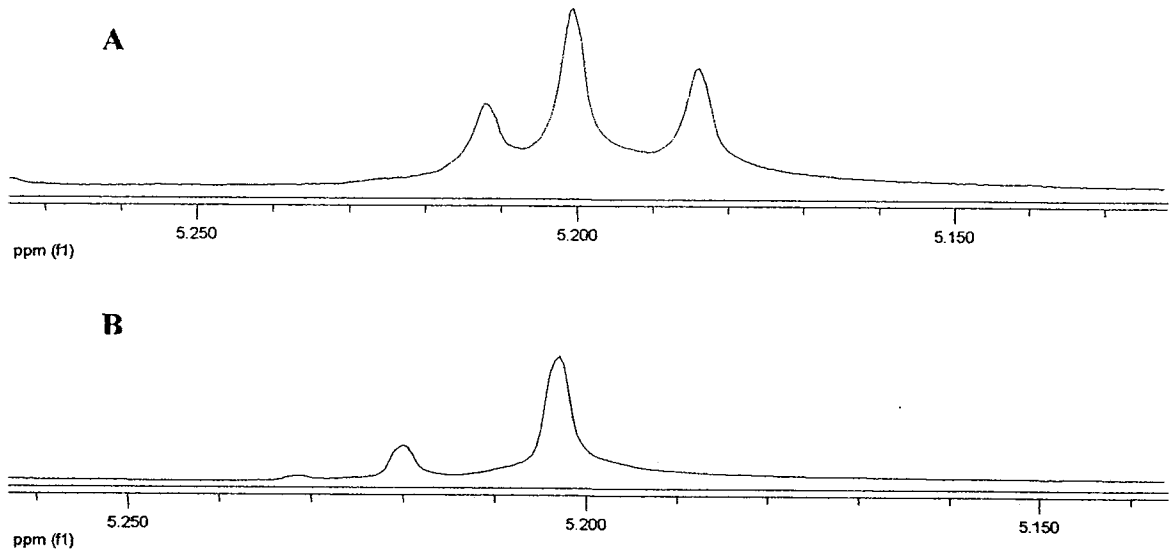

Figure 13: Arene region of the ^{1}H NMR spectrum for the η^6-C_6H_6 ligand of complex 4a′ (A) and 4a′ in the presence of excess chloride ions (B)

4.5 Synthesis and Chemistry of $[RuCl(\eta^6\text{-}C_6H_6)\{P^iPr_2(p\text{-}Ph_3BC_6H_4)\}]_2$, 5

In order to gain a better understanding of the monomer-dimer equilibria observed in **4a-4c** and **4a′-4c**, the effects of adding a chloride scavenger were also explored. Addition of a chloride scavenger should favour the formation of the dimeric species (Scheme 18).

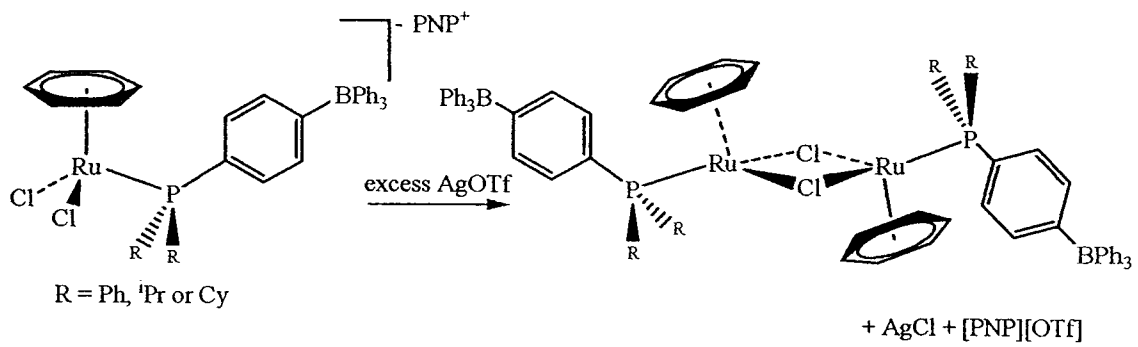

Scheme 18: Synthetic approach to forming compound 5

A sample of compound **4a** was dissolved in THF, followed by the addition of a slight excess of AgOTf. After workup, the ^{1}H and ^{31}P{^{1}H} NMR spectra revealed the reaction proceeded very cleanly. There were two signals found in the ^{31}P{^{1}H} spectrum at δ =

22.1 ppm and δ = 33.2 ppm. The signal at δ = 22.1 ppm was presumed to be the newly formed [PNP][OTf] by-product, and the other signal was tentatively assigned as $[RuCl(\eta^6\text{-}C_6H_6)\{P^iPr_2(p\text{-}Ph_3BC_6H_4)\}]_2$, **5**.

Separating the desired product from the [PNP][OTf] proved to be very difficult. Numerous purification protocols were employed, but were unsuccessful. Eventually, it was determined that the [PNP][OTf] could be separated by careful precipitation out of solution. A spectroscopically purer product was obtained by dissolving the crude reaction mixture in a minimal amount of THF. This was followed by a small portion of hexanes resulting in the formation of a white precipitate. The solution was then filtered and this purification step was repeated to yield only one product, which was characterized via NMR spectroscopy. The $^{31}P\{^1H\}$ NMR spectrum contained only one signal at δ = 33.2 ppm (Figure 14). An equally simple ^1H NMR spectrum of the product revealed one signal attributed to the $\eta^6\text{-}C_6H_6$ region at δ = 5.35 ppm. The phenyl signals ranged from δ = 7.96 ppm to 7.26 ppm. The isopropyl groups of the phosphine had signals at δ = 3.16 ppm, δ = 1.49 ppm and δ = 1.27 ppm (Figure 15). Characterization of the white precipitate via $^{31}P\{^1H\}$, ^1H and ^{19}F NMR spectroscopy provided sufficient information to confidently designate the precipitate as [PNP][OTf]. There were phenyl signals in the ^1H NMR spectrum ranging from δ = 7.36 ppm to 7.22 ppm and one signal found in the $^{31}P\{^1H\}$ NMR spectrum at δ = 22.3 ppm. The ^{19}F NMR spectrum revealed one signal at δ = -75.00 ppm, which is what is expected for OTf [55].

A number of experiments were performed to investigate the reactivity and stability of complex **5**. For example, a variable temperature NMR experiment was conducted to determine whether dimeric compound **5** would dissociate at elevated

temperatures[41,56]. $^{31}P\{^{1}H\}$ NMR spectra for **5** were acquired at 22 °C, 40 °C and 60 °C, however no appreciable changes (e.g. line broadening) were observed as the temperature was raised. The sensitivity of the chloride bridge in **5** towards external ligands was also explored. For example, complex **5** was refluxed in MeCN for 2 hours in an attempt to prepare [RuCl(MeCN)(P^{i}Pr$_2$(*p*-Ph$_3$BC$_6$H$_4$)]. However, the ^{1}H and $^{31}P\{^{1}H\}$ NMR spectra of the product after workup revealed no change. These results are consistent with the variable temperature experiment performed on **5**.

Despite several attempts, analytically pure samples of compound **5** could not be obtained, although spectropically pure sample were obtained. A variety of purification techniques including filtrations, recrystallizations and solvent washes were employed, but all attempts were unsuccessful in acquiring an analytically pure sample.

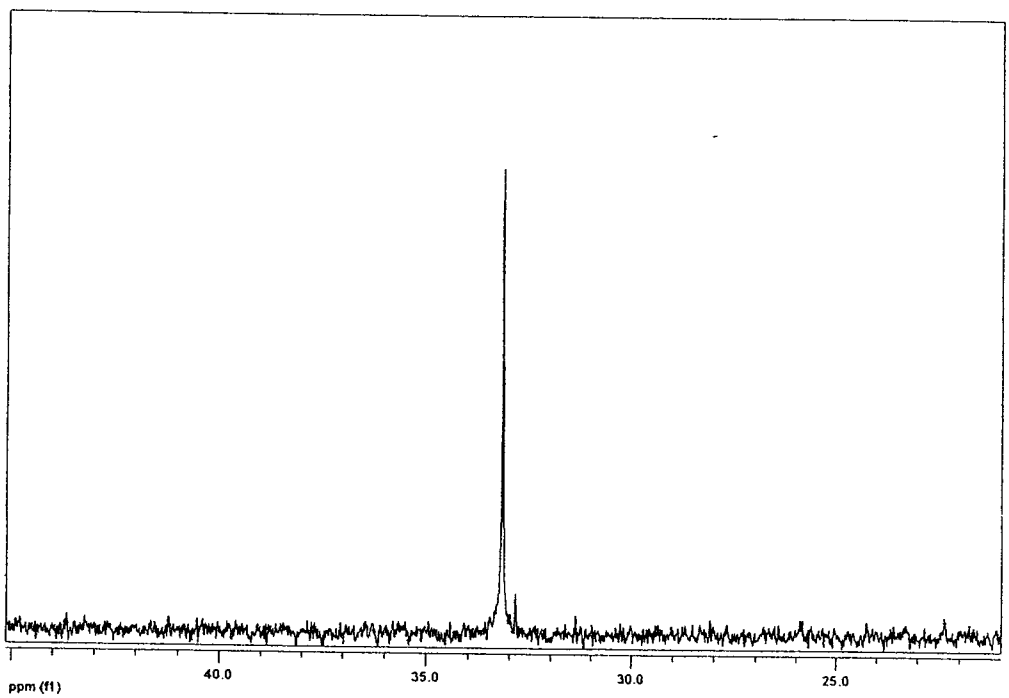

Figure 14: $^{31}P\{^{1}H\}$ NMR spectrum for compound 5

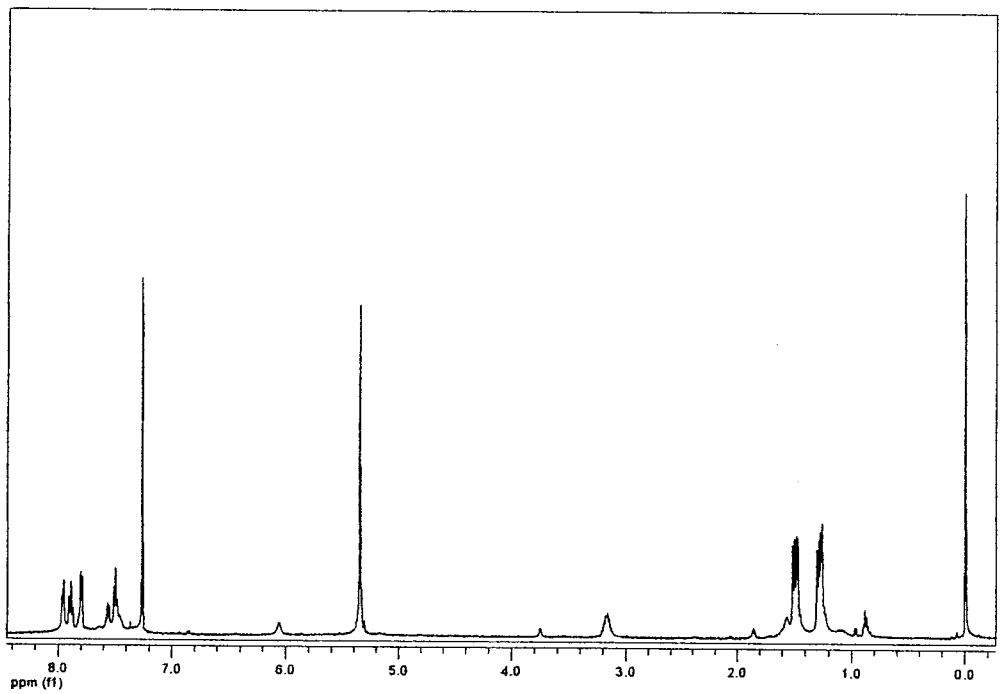

Figure 15: ^{1}H NMR spectrum for compound 5

4.6 Attempted Synthesis of [Ru(MeCN)$_2$(η^6-C$_6$H$_6$){P^{i}Pr$_2$(*p*-Ph$_3$BC$_6$H$_4$)}][OTf]

Investigations into the synthesis of ruthenium-arene-bis(acetonitrile) complexes containing the anionic phosphine were performed. Ruthenium-bis(acetonitrile) complexes are important because of their usefulness as precursors for ligand substitution reactions[57]. Labile acetonitrile ligands of ruthenium-acetonitrile complexes can be replaced in a step-wise manner, making these complexes convenient precursors for a wide range of complexes (Scheme 19). When compound **4a** was treated with two equivalents of AgOTF in the presence of a large excess of MeCN (Scheme 20), the reaction mixture immediately turned yellow and a white precipitate of AgCl formed. Subsequent workup yielded a bright yellow product.

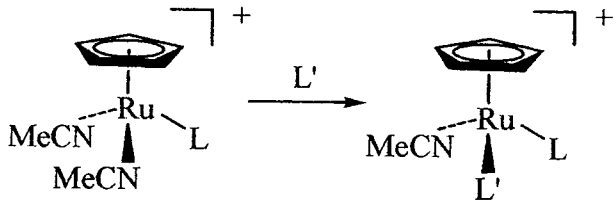

$L = PPh_3$ $L' = py, PMe_3, PCy_3, AsPh_3$

Scheme 19: Example of ruthenium-bis(acetonitrile) complexes serving as precursors to ligand substitution[57a]

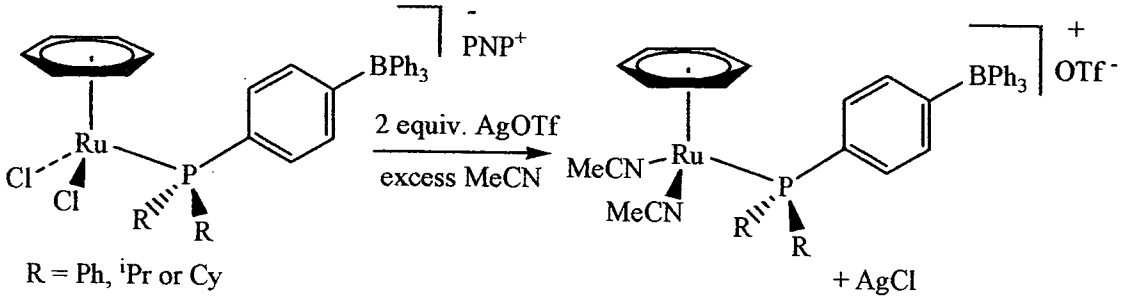

R = Ph, ^{i}Pr or Cy

+ AgCl

Scheme 20: Proposed synthetic strategy to forming $[Ru(MeCN)_2(\eta^6\text{-}C_6H_6)\{P^iPr_2(p\text{-}Ph_3BC_6H_4)\}][OTf]$

Upon analyzing the $^{31}P\{^1H\}$ NMR spectrum, three signals were observed at $\delta = 22.2$ ppm, 39.6 ppm and 36.0 ppm (~4:4.5:1, all singlets). The signal at $\delta = 22.2$ ppm was attributed to [PNP][OTf], whereas the other two signals were tentatively assigned to $[Ru(MeCN)_2(\eta^6\text{-}C_6H_6)\{P^iPr_2(p\text{-}Ph_3BC_6H_4)\}][OTf]$ and $[RuCl(MeCN)(\eta^6\text{-}C_6H_6)\{P^iPr_2(p\text{-}Ph_3BC_6H_4)\}]$. Likewise, the ^1H NMR spectrum revealed two signals in the $\eta^6\text{-}C_6H_6$ region at $\delta = 5.73$ ppm and $\delta = 5.65$ ppm, suggesting two species containing a $\eta^6\text{-}C_6H_6$ ligand. The ^1H NMR spectrum also revealed multiple signals in the acetonitrile region of the spectrum ranging from $\delta = 1.40$ ppm to 1.26 ppm, further supporting the formation of ruthenium-acetonitrile complexes. Numerous purification strategies were employed to isolate the desired product, but were unsuccessful. Several variations to the experimental procedure were employed to increase the yield of the desired product. The ratio of

AgOTf to metal was varied from 2.1 to 5 fold excess, which only resulted in a greater number of unidentified species in the $^{31}P\{^{1}H\}$ NMR spectrum. A number of different halide abstracting agents were used, which included $AgBF_4$, $AgPF_6$ and MeOTf. Increasing the temperature of the reaction to 80 °C was also unsuccessful in increasing yield of the desired product. Varying the phosphine to include the phenyl and cyclohexyl analogues gave similar results.

4.7 Attempted Synthesis of $[Ru(MeCN)_2(\eta^6\text{-}C_6H_6)\{PR_2(p\text{-}Ph_3BC_6H_4)\}][BF_4]$

An alternative approach was employed in order to synthesize the desired ruthenium-arene-bis(acetonitrile) complexes containing the anionic phosphine, this time beginning with $[Ru(\eta^6\text{-}C_6H_6)(MeCN)_3][BF_4]_2$ (Scheme 21).

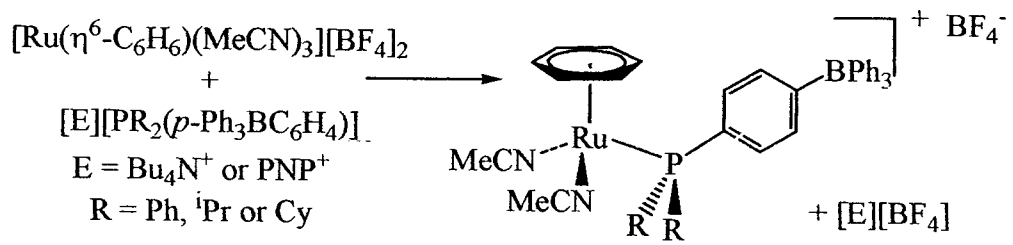

Scheme 21: Proposed synthetic approach to forming $[Ru(MeCN)_2(\eta^6\text{-}C_6H_6)\{PR_2(p\text{-}Ph_3BC_6H_4)\}][BF_4]$

A CH_2Cl_2 solution containing $[Ru(\eta^6\text{-}C_6H_6)(MeCN)_3][BF_4]_2$ was treated with one equivalent of $[PNP][P^iPr_2(p\text{-}Ph_3BC_6H_4)]$, and was allowed to stir for 15 minutes. Following workup, a yellow solid was obtained. The $^{31}P\{^{1}H\}$ NMR spectrum of the solid revealed three signals at δ = 35.7 ppm, 33.3 ppm and 22.2 ppm (~3:1:16.5, all singlets). The signal at δ = 22.2 ppm was attributed to $[PNP][BF_4]$, the signal at δ = 35.7 ppm was attributed to $[Ru(MeCN)_2(\eta^6\text{-}C_6H_6)\{P^iPr_2(p\text{-}Ph_3BC_6H_4)\}][BF_4]$, and the remaining signal could not be assigned confidently. As mentioned in Section 4.6, the

attempted synthesis of $[Ru(MeCN)_2(\eta^6\text{-}C_6H_6)\{P^iPr_2(p\text{-}Ph_3BC_6H_4)\}][OTf]$ revealed a signal in the $^{31}P\{^1H\}$ NMR spectrum at $\delta = 36.0$ ppm. Thus, the similar signals observed in both spectra are likely the same compound and can be tentatively assigned to $[Ru(MeCN)_2(\eta^6\text{-}C_6H_6)\{P^iPr_2(p\text{-}Ph_3BC_6H_4)\}][E]$ (E = OTf or BF_4^-). Within the ^1H NMR spectrum, there are two signals in the $\eta^6\text{-}C_6H_6$ region at $\delta = 5.73$ ppm and $\delta = 5.67$ ppm (~1:1, all singlets). The two signals in the $\eta^6\text{-}C_6H_6$ region suggest there exists two species containing an $\eta^6\text{-}C_6H_6$ ligand. There were a number of MeCN signals found in the ^1H spectrum ranging from $\delta = 1.41$ ppm to 1.27 ppm, suggesting multiple species containing MeCN ligands. Further attempts to purify the product mixture were unsuccessful and extending the reaction time had no affect in yielding only the desired product.

A number of experiments involved varying the anionic phosphine used in the ligand substitution. Using a similar synthetic scheme, $[Li][PPh_2(p\text{-}Ph_3BC_6H_4)]$ was used instead of $[PNP][P^iPr_2(p\text{-}Ph_3BC_6H_4)]$. Allowing the solution to stir for 3 hours, a bright yellow product was obtained. Characterization via $^{31}P\{^1H\}$ NMR revealed the reaction proceeded very cleanly with only one phosphorus containing species found in solution at $\delta = 33.7$ ppm. An equally simple ^1H spectrum was acquired and contained one signal in the $\eta^6\text{-}C_6H_6$ region at $\delta = 5.48$ ppm and one MeCN signal found at $\delta = 1.49$ ppm. A large singlet at $\delta = 5.35$ ppm was also observed which indicates that the product is solvated with a significant amount of CH_2Cl_2. Several different methods of purification were employed including solvent washes, precipitation reactions, ion exchanges and recrystallizations which proved unsuccessful in isolating a pure product.

4.8 Attempted Synthesis of [RuCl(=C=C=CPh$_2$)(η^6-C$_6$H$_6$){P^{i}Pr$_2$(*p*-Ph$_3$BC$_6$H$_4$)}]

In the third phase of the project, attention was turned towards investigating the formation of ruthenium-arene-allenylidene complexes containing the [PR$_2$(*p*-Ph$_3$BC$_6$H$_4$)]$^-$ ligand. There are numerous examples of [RuCl$_2$(η^6-arene)(PR$_3$)] complexes serving as a convenient precursor to ruthenium-allenylidene complexes[58,59]. Ruthenium-allenylidene complexes are known to promote ring closing metathesis[59a,b,c], ring-opening metathesis polymerization[59d] and enyne-metathesis[60]. The general method of synthesizing ruthenium-allenylidenes involves the spontaneous dehydration of a propargyl alcohol after prior coordination to a metal centre[58,59] (Scheme 22).

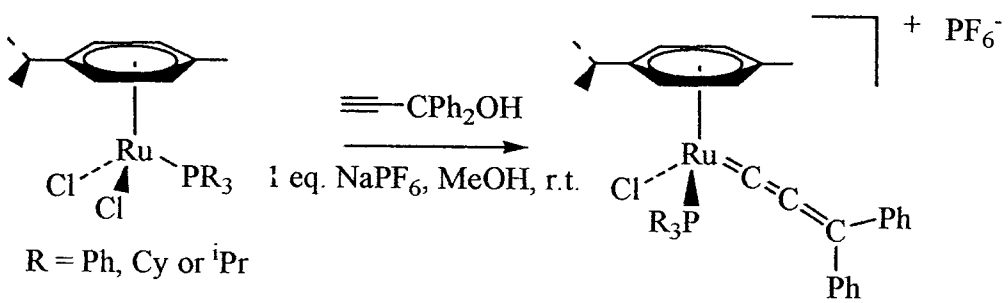

Scheme 22: General method of preparing ruthenium-allenylidenes[59b]

Utilizing a similar synthetic approach, a THF solution containing compound **4a** and 1,1-diphenylpropynol was treated with MeOTf in attempt to form [RuCl(=C=C=CPh$_2$)(η^6-C$_6$H$_6$){PR$_2$(*p*-Ph$_3$BC$_6$H$_4$)}] (Scheme 23). After the addition of the MeOTf, the solution gradually changed colour from a brown solution to a deep, dark red solution, which is encouraging because many ruthenium-allenylidene complexes are often deep red[59]. After 2 hours, the volatiles were removed to yield a red product. The product was then washed with benzene and the red supernatant was cannulated into a dry clean flask, leaving behind an oily brown product.

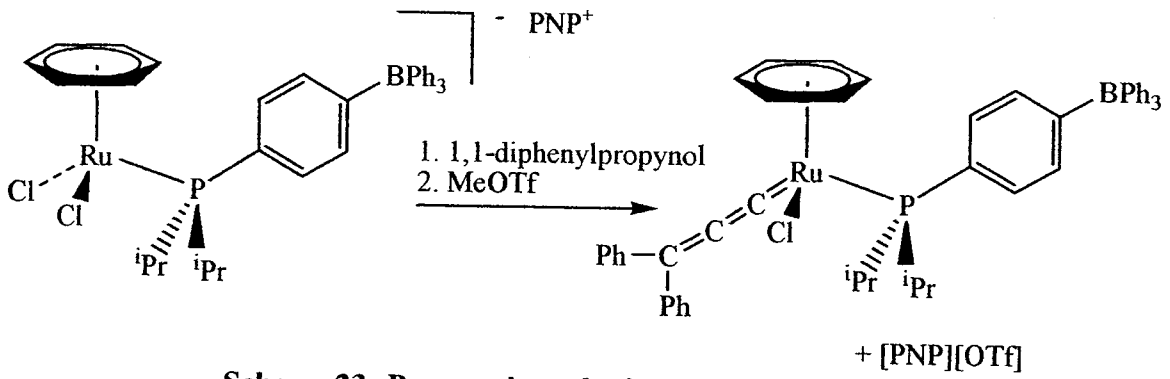

Scheme 23: Proposed synthetic strategy for forming

$[RuCl(=C=C=CPh_2)(\eta^6\text{-}C_6H_6)\{PR_2(p\text{-}Ph_3BC_6H_4)\}]$

Interestingly, the ^1H and $^{31}P\{^1H\}$ NMR spectra for the oily brown product revealed spectra similar to compound **5** and [PNP][OTf]. On the other hand, the $^{31}P\{^1H\}$NMR spectrum for the red product revealed three distinct signals of varying intensities. The most dominant peak at $\delta = 22.3$ ppm was assigned to [PNP][OTf] and the two remaining signals were observed at $\delta = 32.8$ ppm and $\delta = 32.4$ ppm, respectively. The ^1H NMR spectrum revealed two signals in the arene region at $\delta = 4.52$ ppm and $\delta = 4.48$ ppm, indicating two species containing the η^6-C_6H_6 ligand. Acquiring a ^{13}C NMR spectrum of the red product would be diagnotic in determining if the allenylidene formed, however all attempts were unsuccessful because the product decomposed during the acquisition period. Attempts to increase the yield of the desired product were unsuccessful despite numerous variations to the experimental procedure. Variations to the experimental procedure included varying halide abstracting agents to include AgOTf, $AgBF_4$, $AgPF_6$, $AgNO_3$, $NaPF_6$ and NH_4PF_6. The reagent ratios used in the experiment ranged from 1 to 100 fold excess of 1,1-diphenylpropynol to metal and 1 to 1.5 fold excess of halide abstracting agent to metal. Three other solvents were used and include methanol, THF and 1,2-dichloroethane. Finally, the temperature of the reaction was elevated to include

40°C and 80°C, respectively. In most cases, variations to the experimental procedure resulted in a greater number of unidentified species in the $^{31}P\{^{1}H\}$NMR spectrum.

4.9 Attempted Synthesis of [RuCl(=C=CHPh)(η^6-C_6H_6){P^iPr_2(*p*-$Ph_3BC_6H_4$)}]

Despite unsuccessful attempts at forming the allenylidene product, attention was focused on forming ruthenium-arene-vinylidene complexes containing the anionic phosphine ligand. Ruthenium-vinlyidenes are catalytically important complexes[64], and have been known to promote ring closing metathesis[63], ring-opening metathesis[63] and [2+2] cycloaddition reactions[64]. Ruthenium-vinlyidene complexes can be formed by treating [$RuCl_2(\eta^6$-arene)(PR_3)] complexes with a halide abstracting agent in the presence of a substituted alkyne, such as phenylacetylene (Scheme 24).

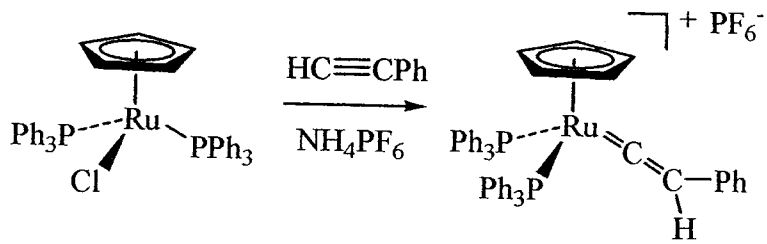

Scheme 24: Example of forming ruthenium-vinylidenes[65]

Following a similar approach, a CH_2Cl_2 solution containing compound **4a** and phenylacetylene was treated with AgOTf, and was allowed to stir for 18 hours (Scheme 25). During this time, the solution colour gradually changed from brown to a slightly lighter brown along with the formation of a white precipitate of AgCl. The solution was filtered and volatiles were removed to yield a brown product. However, the NMR data acquired for the reaction mixture suggested only complex **5** formed. Within the $^{31}P\{^{1}H\}$NMR spectrum, two signals, at δ = 22.3 ppm and δ = 33.1 ppm, were observed.

The signal found at $\delta = 22.3$ ppm was assigned to [PNP][OTf], while the signal found at $\delta = 33.1$ ppm had a similar chemical shift to compound **5**.

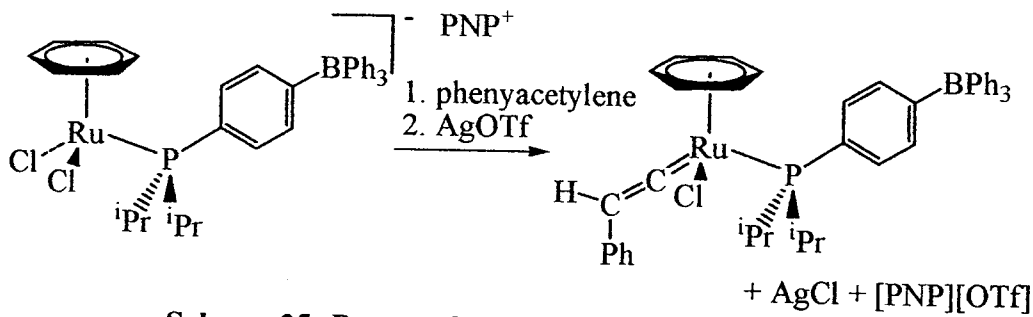

Scheme 25: Proposed synthetic strategy to forming

[RuCl(=C=CHPh)(η^6-C_6H_6){P^iPr_2(*p*-$Ph_3BC_6H_4$)}]

The ^{1}H NMR spectrum was also similar to compound **5**. Furthermore, no signal pertaining to the C_β-H of the vinylidene was observed in the ^{1}H NMR, suggesting the vinylidene did not form. The reaction conditions were altered in an attempt to form the vinylidene product, but all attempts were unsuccessful. The reactant ratios were altered to range from 1 to 10 fold excesses of phenylacetylene to metal and 1 to 1.5 fold excesses of halide abstracting agent to metal, but yielded only complex **5**. Variations to the solvents used in the reaction include methanol, THF and 1,2 dichloroethane and increasing the temperature of the reaction to 40°C and 80°C yielded similar results. Finally, a variety of halide abstracting agents were used and included MeOTf, $AgBF_4$, $AgPF_6$, $AgNO_3$, $NaPF_6$ and NH_4PF_6, but was unsuccessful in forming the vinylidene product. Clearly, compound **5** is a stable complex and forms very rapidly in these reactions.

5. Conclusions

A series of ruthenium-arene complexes containing the anionic phosphines $[PR_2(p\text{-}Ph_3BC_6H_4)]^-$ were synthesized. X-ray crystallographic studies of $[PNP][RuCl_2(\eta^6\text{-}C_6H_6)\{P^iPr_2(p\text{-}Ph_3BC_6H_4)\}]$ confirmed the three-legged piano-stool coordination geometry. NMR spectroscopic analysis of compound $[E][RuCl_2(\eta^6\text{-arene})\{PR_2(p\text{-}Ph_3BC_6H_4)\}]$ ($E = PNP^+$ or Bu_4N^+; arene = *p*-cymene or benzene; R = Ph, ^{i}Pr or Cy) unexpectedly revealed complicated spectra, which was attributed to *in situ* monomer-dimer equilibria facilitated by spontaneous chloride ligand dissociation.

The isolation and characterization of $[RuCl(\eta^6\text{-}C_6H_6)\{P^iPr_2(p\text{-}Ph_3BC_6H_4)\}]_2$ further supported the monomer-dimer scenario. A number of studies involving $[RuCl(\eta^6\text{-}C_6H_6)\{P^iPr_2(p\text{-}Ph_3BC_6H_4)\}]_2$ revealed that the dimeric species is a very stable molecule. For example, the synthesis of $[RuCl(py)(\eta^6\text{-}p\text{-cymene})\{PCy_2(p\text{-}Ph_3BC_6H_4)\}]$ and $[RuCl(MeCN)(\eta^6\text{-}p\text{-cymene})\{PCy_2(p\text{-}Ph_3BC_6H_4)\}]$ required an extremely large excess of trapping ligand in order to suppress the formation of the dimeric species. Reactions containing only a slight excess of trapping ligand resulted in a mixture of products and starting materials. Furthermore, the formation of the dimeric species occurred in all reactions involving the synthesis of ruthenium-arene-allenylidenes and -vinylidenes bearing the anionic phosphine. In both cases, NMR spectroscopic data revealed the presence of the dimeric species even in the presence of an extremely large excess of phenylacetylene or 1,1-diphenylpropynol. These observations suggest the formation of the dimer occurs much quicker than the coordination of allenylidene and vinylidene ligands, and is unreactive once formed.

6. References

1. For a review, see: (a) Dias, P.D.; de Piedade, M.E.M; Simoes, J.A.M., *Coord. Chem. Rev.* **1994**, *135*, 737 For recent examples, see: (b) Daniels, M.; Kirss, R.U., *J. Organomet. Chem.* **2007**, *692*, 1716 (c) Buchowicz, W.; Makal, A.; Wozniak, K., *J. Organomet. Chem.* **2009**, *694*, 3179 (d) Garcia, M.H.; Mendes, P.J.; Robuls, M.P.; Duarte, M.T.; Lopes, N., *J. Organomet. Chem.* **2009**, *694*, 2888
2. Tolman, C.A., *Chem. Rev.* **1977**, *77*, 313
3. For examples, see: (a) Lu, C.C.; Peters, J.C., *J. Am. Chem. Soc.* **2002**, *124* 5272 (b) Betley, T.A.; Peters, J.C., *Angew. Chem. Int. Ed.* **2003**, *42*, 2385 (c) Lu, C.C.; Peters, J.C., *J. Am. Chem. Soc.* **2004**, *126*, 15818 (d) Brown, S.D.; Peters, J.C., *J. Am. Chem. Soc.* **2004**, *126*, 4538
4. Barney, A.A.; Heyduk, A.F.; Nocera, D.G., *Chem. Commun.* **1999**, 2379
5. Betley, T.A.; Peters, J.C., *Inorg. Chem.* **2003**, *42*, 5074
6. For more details, see: (a) Tellers, D.M.; Skoog, S.J.; Bergman, R.G.; Gunnoe, T.B.; Harman, W.D., *Organometallics*, **2000**, *19*, 2428 (b) Curtis, M.D.; Shui, K.B.; Butler, W.M.; Huffman, J.C., *J. Am. Chem. Soc.* **1986**, *108*, 3337
7. Peters, J.C.; Feldman, J.D.; Tilley, T.D., *J. Am. Chem. Soc.* **1999**, *121*, 9871
8. Feldman, J.D.; Peters, J.C.; Tilley, T.D., *Organometallics*, **2002**, *21*, 4050
9. King, R.B.; Bisnette, M.B., J. *Organomet. Chem.* **1973**, *56*, 345
10. Detrich, J.L.; Reinaud, O.M.; Rheingold, A.L.; Theopold, K.H., *J. Am. Chem. Soc.* **1995**, *117*, 11745
11. King, R.B.; Bisnette, M.B.; J. *Organomet. Chem.* **1967**, *8*, 287

12. Dapporto, P.; Midollini, S.; Sacconi, L., *Inorg. Chem.* **1975**, *14*, 1643

13. Thomas, J.C.; Peters, J.C., *Inorg. Chem.* **2003**, *42*, 5055

14. Thomas, J.C.; Peters, J.C., *J. Am. Chem. Soc.* **2003**, *125*, 8870

15. Mankad, N.P.; Peters, J.C., *Chem Commun.* **2008**, 1061

16. Qiao, S.; Hoic, D.A.; Fu, G.C., *J. Am. Chem. Soc.* **1996**, *118*, 6329

17. Dornhaus, F.; Bolte, M.; Derner, H.W.; Wagner, M., *Eur. J. Inorg. Chem.* **2006**, 1777

18. Dornhaus, F.; Bolte, M.; Derner, H.W.; Wagner, M., *Eur. J. Inorg. Chem.* **2006**, 5138

19. Thomas, J.C.; Peters, J.C., *Inorg. Chem.* **2004**, *43*, 8

20. Hoic, D.A.; Davis, W.M.; Fu, G.C., *J. Am. Chem. Soc.* **1996**, *118*, 8176

21. Riley, P.E.; Davis, R.E., *Organometallics*, **1983**, *2*, 286

22. Burkett-St. Laurent, J.C.T.R.; Haines, R.J.; Nolte, C.R.; Steen, N.D.C.T., *Inorg. Chem.* **1980**, *19*, 577

23. Codding, P.W.; Kerr, K.A., *Acta. Crystallogr. Sect. B*, **1978**, *34*, 3785

24. Codding, P.W.; Kerr, K.A., *Acta. Crystallogr. Sect. B*, **1979**, *35*, 1261

25. Burford, N., *Coord. Chem. Rev.* **1992**, *112*, 1

26. For a review on ruthenium catalysis, see: (a) Noato, T.; Takaya, H.; Murahashi, S.I., *Chem. Rev.* **1998**, *98*, 2549 (b) Trost, B.M.; Toste, F.D.; Pinkerton, A.B., *Chem. Rev.* **2001**, *101*, 2067

27. For a review on ruthenium-arene complexes, see: Therrien, B., Coord. *Chem. Rev.* **2009**, 493

28. For examples, see: (a) Baratta, W.; De Zotto, A.; Rigo, P., *Organometallics*, **1999**, *18*, 5091 (b) Chaplin, A.B.; Fellay, C.; Laurenczy, G.; Dyson, P., *Organometallics*, **2007**, *26*, 586 (c) Slugovc, C.; Sapunov, V.N.; Wiede, P.; Mereiter, K.; Schmid, R.; Kirchner, K., *J. Chem. Soc., Dalton Trans.* **1997**, 4209 (d) Becker, E.; Slugovc, C.; Ruba, E.; Standfest-Hauser, C.; Mereiter, K.; Schmid, R.; Kirchner, K., *J. Organomet. Chem.* **2002**, *649*, 55 e) Soleimannejad, J.; White, C., *Organometallics*, **2005**, *24*, 2538

29. Bennett, M.A.; Smith, A.K., *J.C.S. Dalton*, **1974**, 233

30. For a review on chromium-arene complexes in organic synthesis, see: Rosillo, M.; Dominguez, G.; Perez-Cestells, J., *Chem. Soc. Rev.* **2007**, *36*, 1589

31. For a review on ruthenium-arene catalysis, see: Rigby, S.H.; Kondratenko, M.A., *Topics Organomet. Chem*, **2004**, *7*, 181.

32. For examples, see: (a) Chaplin, A.B.; Dyson, P., *Organometallics*, **2007**, *26*, 2447 (b) Daguenet, C.; Scopelliti, R.; Dyson, P., *Organometallics*, **2004**, *23*, 4849 (c) Carmona, D.; Lamata, M.P.; Viguri, F.; Ferrer, J.; Garcia, N.; Lahoz, F.J.; Martin, M.L., Oro, L.A.; *Euro. J. Inorg. Chem.* **2006**, 3155

33. O'Connor, J.M.; Friese, S.J.; Rodgers, B.L., *J. Am. Chem. Soc.* **2005**, *127*, 15342

34. For examples, see: (a) Kundig, E.P.; Kondratenko, M.; Romanens, P., *Angew. Chem. Int. Ed.* **1998**, *37*, 3146 (b) Kotch, T.G.; Lees, A.J., *Chem. Mater.*, **1995**, *7*, 801

35. Yu, C.B.; Xia, Y.Q.; Tian, X.H.; Zhou, X.G.; Fan, G.Y.; Li, R.X.; Li, X.J.; Tin, K.C.; Wong, N.B., *J. Organomet. Chem.*, **2006**, *691*, 499

36. Chen, Y.; Valentini, M.; Pregosin, P.S.; Albinati, A., *Inorg. Chim. Acta*, **2002**, *327*, 4

37. Werner, H.; Werner, R., *Chem. Ber.* **1982**, *115*, 3766

38. Yamamoto, Y.; Miyauch, F., *Inorg. Chim. Acta*, **2002**, *334*, 77

39. Zelonka, R.A.; Baird, M.C., *Can. J. Chem.*, **1972**, *50*, 3063

40. Vock, C.A.; Dyson, P.J., *Z. Anorg. Allg. Chem.* **2007**, *633*, 640

41. Tenorio, M.J.; Puerta, M.C.; Valerga, P., *J. Organomet. Chem.* **2000**, *609*, 161

42. Bennett, M.A.; Huang, T.N.; Matheson, T.W.; Smith, A.K., *Inorg Synth.* **1982**, *21*, 74

43. Beach, M.T; Walker, J.M.; Larocque, T.G.; Deagle, J.L., Wang, R.; Spivak, G.J., *J. Organomet. Chem.* **2008**, *693*, 2921

44. SHELXTL (Version 6.14., **2000**), XPREP (Version 2005/2, **2005**), SAINT (Version 7.23A, **2005**), APEX2 (Version 2.0-2, **2006**), Bruker AXS Inc., Madison, Wisconsin, USA.

45. Cromer, D. T.; Waber, J. T., *International Tables for X-ray Crystallography*; Kynoch Press: Birmingham, UK, **1974**; Vol. *4*, Table 2.2 A.

46. For examples, see: (a) Govindaswamy, P.; Mozharivsky, Y.A.; Kollipara, M.R., *Polyhedron*, **2004**, *23*, 3115 (b) Tan, W.; Zhao, X.; Yu, Z., *J. Organomet. Chem.* **2007**, *692*, 5395 (c) Rodriguez, L.I.; Rossell, O.; Seco, M.; Muller, G. *J. Organomet. Chem.* **2007**, *692*, 851 (d) Goux, J.; Le Gendre, P.; Richard, P.; Moise, C., *J. Organomet. Chem.* **2005**, *690*, 301

47. Daniel, T.; Werner, H., *J. Chem. Soc. Dalton Trans.* **1994**, *2*, 221

48. For examples, see: (a) Schutte, R.P.; Rettig, S.J.; James, B.R., *Can. J. Chem.* **1996**, 2064 (b) Griffin, G.E.; Thomas, W.A., *J. Chem. Soc.* B, **1970**, 477

49. For examples, see: (a) Katayama, T.; Onitsuka, K.; Takahushi, S., *J. Organomet. Chem.* 2000, *610*, 31 (b) Zhang, H.-J.; Demerseman, B.; Xi, Z.; Bruneau, C., *Eur. J. Inorg. Chem.* **2008**, 3212

50. For examples, see: (a) de los Rios, I.; Tenorio, M.J.; Tenorio, M.A.J.; Puerta, M.C.; Valerga, P., *J. Organomet. Chem.* **1996**, *525*, 57 (b) Canivet, J.; Brelot, L.K.; Suss-Fink, G., *J. Organomet. Chem.* **2005**, *690*, 3202 (c) Therrien, B.; Suss-Fink, G.; Govindaswamy, P.; Said-Mohamed, C., *Polyhedron*, **2007**, *26*, 4069 (d) Gupta, G.; Yap, G.P.A.; Therrien, B.; Rao, K.M., *Polyhedron*, **2009**, *28*, 844

51. For examples, see: (a) Paris, S.I.M.; Lemke, F.; Somner, R.; Lonnecke, P.; Hey-Hawkins, E., *J. Organomet. Chem.* **2005**, *690*, 1807 (b) Maroni, G.; Baier, H.; Heinemann, F.W.; Pinto, P.; Pritzkon, H.; Zenneck, U., *Inorg Chim Acta*, **2003**, *352*, 188

52. Elsegood, M.R.J.; Tocher, D.A., *Polyhedron*, **1995**, *14*, 3147

53. (a) Therrien, B.; Suss-Fink, G., *Inorg. Chim. Acta.* **2006**, *359*, 4350 (b) Moldes, I. de la Encarncion, E.; Ros, J.; Alvarez-Larena, A.; Piniella, J.F., *J. Organomet. Chem.* **1998**, *566*, 165

54. For examples, see: Crochet, P.; Fernandez-Zumel, M.A.; Beauquis, C.; Gimeno, J., *Inorg. Chim. Acta.*, **2003**, *356*, 114 (b) Tribo, R.; Munoz, J.; Pom, J.; Yavex, R.; Alvarez,-Larena, A.; Pireilla, J.F.; Ros, J., *J Orgomet. Chem*, **2005**, *690*, 4072

55. For examples, see: (a) Cornet, S.M.; May, I.; Redmon, M.P.; Selvage, A.J.; Sharrard, C.A.; Rosnel, O., *Polyhedron*, **2009**, *28*, 363 (b) Hayashida, T.; Kondo, H.; Terasawa, J.; Kirchner, K.; Sunada, Y.; Nagashima, H., *J. Organomet. Chem.* **2007**, *692*, 382

56. (a) Kuo, C.-N.; Huang, T.-Y.; Shao, M.-Y.; Gau, H.-M., *Inorg. Chim. Acta*, **1999**, *293*, 12 (b) Perdih, F.; Pevec, A.; Petricek, S.; Petric, A.; Lah, N.; Kogej, K.; Demsar, A., *Inorg. Chem.* **2006**, *45*, 7915

57. (a) Ruba, E.; Semanko, W.; Maithner, K.; Soldouzi, K.M.; Slugovc, C.; Mereiter, K.; Schmid, R.; Kirchner, K., *Organometallics*, **1999**, *18*, 3843 (b) Demerseman, B.; Renaud, J.L.; Toupet, L.; Hubert, C.; Bruneau, C., *Eur. J. Inorg. Chem.* **2006**, 1371 (c) Gill, T.P.; Mann, K.R., *Organometallics*, **1982**, *1*, 485 (d) Becker, E.; Slugovc, C.; Ruba, E.; Standfest, Hauser, C.; Mereiter, K.; Schmid, R.; Kirchner, K., *J. Organomet. Chem.* **2002**, *649*, 55

58. For reviews on ruthenium allenylidenes, see: (a) Winter, R.F.; Zalis, S., *Coord. Chem. Rev.* **2004**, *248*, 1565 (b) Rigaut, S.; Touchard, D.; Dixneuf, P.H., *Coord. Chem. Rev.* **2004**, *248*, 1585 (c) Dragutan, I.; Dragutan, V., *Platinum Metals Rev.* **2006**, *50*, 81

59. (a) Picquet, M.; Touchard, D.; Bruneau, C.; Dixneuf, P.H., *New J. Chem.* **1999**, 141 (b) Furstner, A.; Liebl, M.; Lehmann, C.W.; Picquet, M.; Kunz, R.; Bruneau, C.; Touchard, D.; Dixneuf, P.H., *Chem. Eur. J.* **2000**, *6*, 1847 (c) Ghebreyessus, K.Y.; Nelson, J.H., *Inorg. Chim. Acta.*; **2003**, *350*, 12 (d) Castarlenas, R.; Semeril, D.; Noels, A.F.; Demonceau, A.; Dixneuf, P.H., *J. Organomet. Chem.*, **2002**, *663*, 235

60. Buriez, B.; Burns, I.D.; Hill, A.F.; White, A.J.P.; Williams, D.J.; Walton-Ely, J.D.E.T., *Organometallics*, **1999**, *18*, 1504

61. Selegue, J.P., *Organometallics*, **1982**, *1*, 218

62. For reviews on ruthenium vinylidenes, see: (a) Katayama, H.; Ozawa, F., *Coord. Chem. Rev.* **2004**, *248*, 1703 (b) Puerta, M.C.; Valerga, P., *Coord. Chem. Rev.* **1999**, *193*, 977 (c) Dragutan, I.; Dragutan, V., *Platinum Metals Rev.* **2004**, *48*, 148

63. (a) Katayama, H.; Urushima, H.; Ozawa, F., *J. Organomet. Chem.*, **2000**, *606*, 16 (b) Opstal, T.; Verpoort, F., *J. Mol. Cat. A: Chem.*, **2003**, *200*, 49

64. Onitsuka, K.; Katayama, H.; Sonogashira, K.; Ozawa, F., *J. Chem. Soc. Chem Commun.*, **1995**, 2267

65. Bruce, M.I.; Wallis, R.C., *Aust. J. Chem.*, **1979**, *32*, 1471